Inkjet printing for flexible electronics: Materials, processes and equipments

ARTICLE *in* CHINESE SCIENCE BULLETIN · OCTOBER 2010

Impact Factor: 1.58 · DOI: 10.1007/s11434-010-3251-y

Review

Chinese Science Bulletin

SPECIAL TOPIC: Huazhong University of Science and Technology Mechanical Engineering

October 2010 Vol.55 No.30: 3383–3407
doi: 10.1007/s11434-010-3251-y

Inkjet printing for flexible electronics: Materials, processes and equipments

YIN ZhouPing*, HUANG YongAn*, BU NingBin, WANG XiaoMei & XIONG YouLun

State Key Laboratory of Digital Manufacturing Equipment and Technology, Huazhong University of Science and Technology, Wuhan 430074, China

Received October 20, 2009; accepted February 5, 2010

Inkjet printing, known as digital writing technique, can directly deposit functional materials to form pattern onto substrate. This paper provides an overview of inkjet printing technologies for flexible electronics. Firstly, we highlight materials challenges in implementing flexible devices into practical application, especially for inkjet printing process. Then the micro/nano-patterning technologies of inkjet printing are discussed, including conventional inkjet printing techniques and electrohydrodynamic printing techniques. Thirdly, the related equipments on inkjet printing are shown. Finally, challenges for its future development are also discussed. The main purpose of the work is to condense the basic knowledge and highlight the challenges associated with the burgeoning and exciting field of inkjet printing for flexible electronics.

flexible electronics, nanomanufacturing, organic thin film transistor, micro/nano-patterning, inkjet printing, electrohydynamics, roll-to-roll

Citation: Yin Z P, Huang Y A, Bu N B, et al. Inkjet printing for flexible electronics: Materials, processes and equipments. Chinese Sci Bull, 2010, 55: 3383–3407, doi: 10.1007/s11434-010-3251-y

1 Overview of flexible electronics technology

Flexible electronics, also known as printable/organic electronics, represent a technology for building electronic circuits by depositing electronic devices onto flexible substrates. Realization of flexible electronics with performance equal to conventional microelectronics built on brittle semiconductor wafers, but in high mobilities, optical transparency, light-weight, stretchable/bendable formats and easy to print rapidly over large areas would enable many new applications [1–4] not satisfied by a traditional rigid electronics. The applications vary from medicine and biology to energy technology and space science [1,2], such as flexible display [4,5], thin film solar cell [6,7], large area sensors and actuators [8,9], shown in Figure 1. These applications are based on thin film transistors (TFTs) which have strong materials and processes contents. Flexible electronics have open boundaries that move with its development and applications and is a highly interdisciplinary field. As a result, there are considerable opportunities for innovation and basic scientific research into new types of electronic materials, processes and equipments.

The flexibility, a critical issue in flexible electronics, is one of the most important differences from traditional microelectronics. Polymer organics and inorganic materials are the two kind of materials adopted in flexible electronics. The polymer organics are generally believed to be well suited for these applications and naturally compatible with polymeric substrates. However, the electrical properties is not ideal when devices are fabricated with polymer organics. This leads to interest in the possibility of inorganic based flexible electronics [10]. It is a challenge to design a bendable and stretchable electronics based on inorganic materials due to their small fracture strain. The most basic realization is thin films of the inorganics are adopted as semiconductors, conductors and/or insulators on substrates to mini-

*Corresponding authors (email: yinzhp@mail.hust.edu.cn, yahuang@hust.edu.cn)

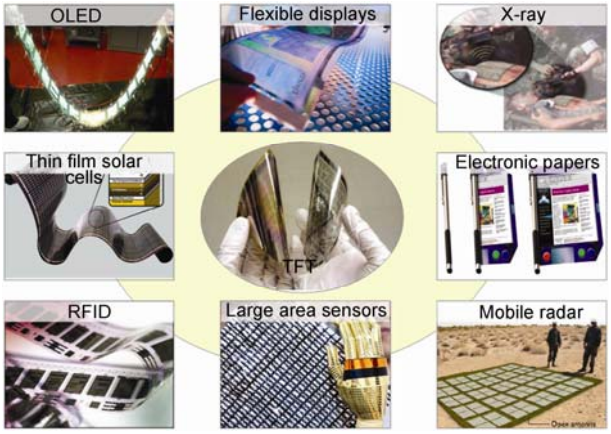

Figure 1 Flexible TFT arrays enabling technologies for a whole range of novel applications.

mize the strains induced by bending or stretching. Plentiful studies on mechanics are devoted into bendability, stretchability, duality and cracking behavior. The bending of inorganic electronic materials on plastic substrates was theoretically and experimentally studied, and the interfacial peeling stress and shear stress were also given [11]. An approach based on buckling behavior was developed to circumvent the limitations of stretchability and the low flexural rigidity of flexible integrated circuits [12–16]. Circuits in wavy patterns offer fully reversible stretchable/compressibility without substantial strains in the circuit materials themselves. Some studies have shown that the wavy can be controlled in micro- and nanoscale systems to generate interesting structures with well defined geometries and dimensions in 100 nm to 100 μm range [17], and their stretchability can be improved by controlling the buckles' orientation, amplitude and wavelength [18]. Freestanding Si/metal thin films rupture when stretched beyond 1%–2% [19]. However, bonded to a plastic substrate, they can sustain plastic deformation ten times larger than its fracture strain, yet remain electrically conductive [14,20]. Xu et al. reviewed the flexible electronics system and their mechanical properties [21]. The authors studied the design-for-reliability of the flexible electronics based on temperature-dependent properties, gave the buckling behavior related with the temperature, and calculated the critical working temperature [22,23].

Flexible electronics manufacturing includes: Preparation of materials → deposition → patterning → encapsulation which can be integrated on roll-to-roll (R2R) web. The flexibility of the flexible electronics leads to lots of characteristics and chance for manufacturing process. Figure 2 shows a simple conceptual illustration of the production of flexible electronics devices based on R2R manufacturing process [24]. The major considerations for flexible electronics are cost, throughput, achievable feature size, and compatibility with organic materials. Flexible electronics manufacturing has largely been neglected until recently,

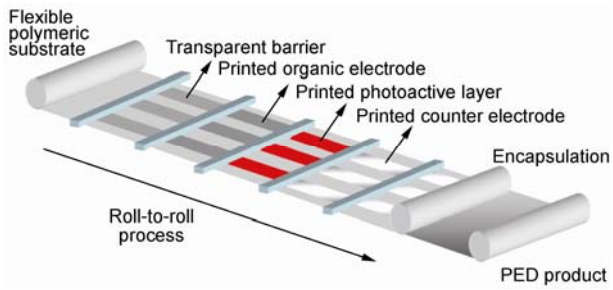

Figure 2 Schematic representation of a future R2R process for flexible electronics manufacturing [24].

primarily because active materials and patterning techniques have only recently emerged from the realm of pure research into the very early development stages but potentially large industry in the future.

High-resolution patterning techniques for defining the channel length between the source and drain electrodes are critical for fabrication of TFTs due to its influences on current output, the switching speed and so on. Specifically, patterning of organic semiconductors is necessary to eliminate parasitic leakage and reduce cross talk to achieve high on-off ratios. The channel length needs to be less than 10 μm for most applications with OTFTs (Organic Thin Film Transistors). Various patterning techniques have been developed, including optical lithography, shadow masking, and printing (micro-contact printing and inkjet printing), whose comparison is listed in Table 1. Optical lithography and other conventional techniques are well-developed for the patterning of microelectronic devices. Although they have high resolution, they are not well suited to flexible electronics because their process is very complex, expensive, time consuming, materials wasting, and only suitable for patterning of small areas, and requires many steps with resists, solvents and developers uncompatible with plastic substrates [25]. Moreover, the harsh conditions required for etching the underlying layers and removing the photo-resist destroys the activity of most organic electronic materials and polymeric substrates [24]. More detail discuss on light-based patterning techniques for organic electronics can refer to [26]. Shadow mask patterning is a "dry" process avoiding solvents which could degrade the organic semiconductors. However, its resolution is limited.

The development of direct printing of functional materials has attracted considerable attention as a patterning technology for flexible electronics. Printing methods implement depositing and patterning materials in one single step. There are mainly two kinds of printing methods: (1) Transfer and bonding of completed circuits to a flexible substrate, such as transfer printing; (2) fabrication of the circuits directly on the flexible substrate, such as inkjet printing and micro- contact printing (soft lithography) [26]. In transfer printing, the whole structure is fabricated by standard methods on a Si wafer or a glass plate then transferred to a flexible substrate, which have the advantage of providing high-performance

Table 1 Comparison of several typical patterning technologies

	Photolithography	Shadow mask	Micro-contact printing	Inkjet printing
Cost	Extremely high	Low	Medium	Low
Area	Extremely small	Large	Medium	Large
Efficiency	Low	High	High	High
Temperature	High	Low	Medium	Low and High
Mask	Needed	Needed	Needless	Needless
Resolution	Extremely high	Low	High	High
Compatibility with polymer	Bad	Good	Bad	Excellent
Flexibility	Bad	Bad	Bad	Good, digital lithography
Compatibility with R2R	Bad	Medium	Good	Good
Material consume	Large	Medium	Low	Low
Requirement of environment	Clean rooms, vibration isolation	Low	Medium	Low
Process	Multi-step	Multi-step	Multi-step	All in one
Mode of action	Noncontact	Contact	Contact	Noncontact

devices on flexible substrates. It mainly benefits from high-resolution lithography and high-temperature deposit technology. Its drawbacks are small surface area coverage and high cost comparable with optical lithography [1]. Micro-contact printing creates multi-level patterns used as masks, and is compatible with high-throughput batch or R2R technology. One master can produce perhaps more than 100 stamps, and each stamp lasts over 3000 imprints, so the imprint stamp costs per imprint are comparably low [1]. It is capable of producing excellent resolution as small as 60 nm at rates of centimeters per second, but it is relatively difficult to pattern multiple layers [27]. Lan et al. [28] have given an excellent review on template fabrication for nanoimprint lithography, where several kinds of nanoimprint techniques are discussed in detail. Micro-contact printing can be adopted for many materials, such as a-Si, poly-Si, and TMOs (Transition Metal Oxides) in spite of organic material.

Pattern processes for flexible electronics should ideally allow: Noncontact patterning, low temperature process, additive patterning, real-time adjustment, three-dimensional structuring, easy to registration, printability of organics/inorganic materials, low cost, compatible with large area and high-throughput processing. It can be noted from Table 1 the inkjet printing process has the potential to reach all the above requirements. Inkjet printing as digital lithography is a promising method to directly writing solution-processable materials at room temperature [29,30], which is the first step in simplifying the fabrication. In a second step, solution-processable semiconductors and metals can be used to replace conventional vacuum deposited materials. It may reduce the cost as low as a few dollars per square meter [2]. Inkjet printing method has several unique advantages: (1) The pattern quality is no longer limited by the depth of focus of the optics. Patterning on non-planar surfaces, even deep trenches becomes possible [30]. (2) It has excellent compatibility with organic and inorganic materials, which makes it different from other printing techniques. (3) As a data driven process, it directly fabricate devices from CAD/CAM. It can register dynamically over large areas and real-time align. (4) As a noncontact patterning, it can minimize contamination. Imperfections such as localized and layer-to-layer distortion are identified and corrected within a virtual mask before patterning. (5) It provides a drop-on-demand (DOD) digital lithographic process without physical masks and material is only applied where it is needed. (6) It allows one to design and rapidly fabricate microstructure with complex three-dimensional shapes. And the microstructure can be changed rapidly through software-based printer-control systems.

The main purpose of the work is to condense the basic knowledge needed to understand the various technologies associated with the burgeoning and exciting field of inkjet printing for flexible electronics. Materials, processes and equipments are highlighted to show the manufacturability of flexible electronics. Even so, this paper is hard to review various aspects of materials, processes and equipments for inkjet printing technology.

2 Materials for inkjet printing

2.1 Evaluation of materials' printability

Figure 3 shows the structure of a typical OLED (Organic Light-Emitting Diode) device consisting of flexible substrates, transparent barrier layers, electrode layers, semiconductive layers and light-emitting layer [24]. The application of inkjet printing for patterning various devices requires functional inks holding special properties. In addition to the widely-discussed electrical properties, such as mobility, on-off voltage, threshold voltage stability [31,32], the materials' printability plays critical roles in inkjet printing. Firstly, the "ink" must have the capability of being stably and accurately printed to directly pattern maskfreely. Secondly, the "ink" has to meet strict physicochemical properties, such as viscosity and surface tension, to achieve the best printed pattern, optimal performance and reliability. Structure at both molecular- and nano-scale will impact attributes such as morphology (surface roughness, grain size), adhesion, mechanical integrity, solubility, and chemical and environmental stability. These factors, in turn, will affect device performance, notably electrical performance (mobility, conductivity, on/off ratio, threshold voltage) [33].

The interrelationship between inkjet printability and

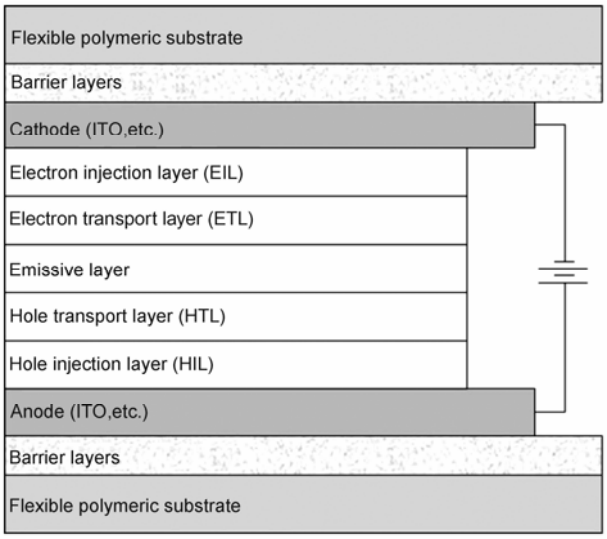

Figure 3 Schematic representation of the structure of a flexible OLED device [24].

physical and rheological properties of the ink have been investigated for non-Newtonian fluids, including velocity (v), characteristic length(α), viscosity (η), density (ρ), and surface tension (γ) [34], in addition viscoelastic properties and yield stress under shear and compression [26]. Reynolds number, $N_{Re}=v\alpha\rho/\eta$, is the ratio of inertial to viscous forces, and the Weber number, $N_{We}=v^2\alpha\rho/\eta$, is a balance between inertial and capillary forces [35]. Still other dimensionless groups can be used to incorporate the effects of viscoelasticity, such as the Weissenberg number $W_i=\lambda v/\alpha$ where λ is the characteristic relaxation time of the fluid [36]. The follows would be obtained:

$$Z=\frac{(\alpha\rho\gamma)^{\frac{1}{2}}}{\eta}=\frac{N_{Re}}{(N_{We})^{\frac{1}{2}}}. \quad (1)$$

The spreading behavior of the inks is determined by the hydrodynamic properties (N_{Re} and N_{We}). The printability was determined using the inverse (Z) of the Ohnesorge number which relates to the viscosity, surface tension, and density of the fluid. Jang et al. [34] observed: When $2<Z<4$, the tail had a sufficiently fast relative velocity to catch up to the droplet head, and merged with the head without a secondary rupture of the filament from the droplet. In the case of $6<Z<13$, it was occurred that a secondary rupture of the elongated filament from the falling droplet head, because the surface tension drive minimization of the surface area. But the tail velocity remained fast enough to recombine with the primary droplet during the filament recoil stage. When $Z>14$, inks were easily ejected by the applied pressure without significant viscous dissipation. The primary droplet fell with a high relative travel velocity, so that the separated tail which formed transient satellites could not catch up with the droplet head. The large oscillatory kinetic energy and the high surface tension tend to induce a secondary rupture, which generated a primary droplet and permanent satellites. So fluids with $Z>14$ are not printable fluids.

The surface tension should be higher than 30 mN/m and the pressure low enough to prevent dripping of the ink from the nozzle [26]. Firstly, to generate droplets with micro-scale diameters, sufficiently high kinetic energies (for example, 20 μJ for HP 51626A) and velocities (normally 1–10 m/s) are necessary to exceed the interfacial energy that holds them to the liquid meniscus in the nozzle. Printing high-viscosity materials is difficult for conventional inkjet printing but electrohydrodynamic (EHD) printing, as the power generated by the piezoelectric and heater membrane is limited [37]. The viscosity should be sufficiently low (Table 2) to allow the channel to be refilled in about 100 μs [27]. Secondly, high evaporation rates in the inks can increase the viscosity locally at the nozzles. The solvent volatility should be sufficiently low in order to avoid clogging. Two important solution parameters are listed for several typical inkjet printing system in Table 2, but not limited by these parameters.

2.2 Inorganic materials for inkjet printing

The printable inorganic material includes metal and nonmetal, such as carbon nanotubes for transparent conductors, transition metal oxide for semiconductors and dielectrics, metal nanoparticles for electrodes, and so on. All the above materials are able to build flexible electronics by inkjet printing.

(i) Carbon nanotube. Single-wall/multi-wall carbon nanotubes (SWCNTs/MWCNTs) hold many kinds of advantageous physical properties [38] such as excellent thermal conductivity, good mechanical strength, optional semiconducting/metallic nature, and advanced field-emission behavior. Fan et al. [39] and Tong et al. [40] have printed thin films based on MWCNT-based ink and a solution ink of MWCNTs dissolved in water, respectively. The results showed that: For the first printed layer, both inks cannot form good conductive network. With the increase of printed layers, continuous MWCNTs conductive network were formed gradually, which exponentially decreased the electrical resistance. When the films are printed by three layers of MWCNT-based ink and four layers of solution ink of MWCNTs with sub-100 nm thick, the networks are com-

Table 2 Typical parameters of solution for inkjet printing

	Piezo-DOD	Thermal-DOD	E-Spinning	E-Spraying	EHD jetting
Viscosity (mP S)	<40	1.28	7–175	2.76	–90
Surface tension (mN/m)	20–70	Temperature-depended	15–64	–45	–50

pact and consecutive enough to cover almost all holes and voids on the paper (Figures 4 and 5). The electrical resistance of the strips hardly decreases with the further increase of printing times. Song et al. [41] printed films of SWCNTs by inkjet printing which are pure SWCNTs dispersed in dimethyl. The film is both conductive and transparent. Mabrook et al. [38] fabricated the thin films containing SWCNTs using inkjet printing. The films exhibit nonlinear current versus voltage behavior which could be fitted to the theoretical model for Poole-Frenkel conductivity.

MWCNTs are successfully embedded in polymer nanofibers (PEO) fabricated by electrospinning [42]. Initial dispersion of MWCNTs in water was achieved using amphiphiles, either small molecules (sodium dodecyl sulfate) or polymers (Gum Arabic). These dispersions provided separation of MWCNTs and their individual incorporation into PEO nanofibers by subsequent electrospinning. Zhang et al. [43] functionalized MWNTs by grafting Triton X-100 on their surface to improve their dispersion in a solution of polyacrylonitrile (PAN) matrix. Well-aligned composite nanofibres containing PAN and MWCNTs were prepared by electrospinning in dimethyl formamide solution. The nanofibres, with diameters of 100 nm, can be uniaxially aligned across the gap between the parallel electrodes. Figure 6 shows the individual surface-functionalized MWNTs are embedded within the nanofibres.

(ii) Metal nanoparticles. Many kinds of metal nanoparticles such as gold (Au), silver (Ag) and copper (Cu) are employed for producing conductive ink, which can be divided into three kinds of inks, suspensions of metallic nanoparticles which have low sintering temperature due to their small sizes [44–46], solutions of metallo-organic precursors which can be converted to metal at low temperature [47] and use solutions of metal compound which can be converted to silver at high temperature(> 400°C) [48].

Park et al. [49] have developed a conductive ink containing 40–50 nm copper particles. Cu nanoparticles synthesized by polyol process from which well-dispersed conductive ink with low viscosity is prepared. Copper patterns printed by inkjet printing exhibited metal-like appearance. Woo et al. [50] have developed ink by adding different-size Ag nanoparticles with a mean size of 20 nm which significantly improve the particle packing density up to 86% by filling the pores between the larger Cu particles with a mean size of 65 nm at the ratio of Cu/Ag=3∶1. The ink facilitates better conductivity than pure Cu metal film. Importantly, this mixed metal-based conductive ink allows us to directly write conductive features on transparent plastic substrates such as polyethersulphone at sufficiently low temperature (175–210°C).

Silver has gained more interest. The finely dispersed silver nanoparticle is gaining comprehensive applications, such as catalyst, transparent conductive coating, active ink for electronics, due to the unique properties such as chemical stability, catalytic activity and excellent electric conductivity. For successful application and commercialization, silver nanoparticles dispersion in water inks adopted by inkjet printing technique have to meet the following [51]: a simple and inexpensive method for nanoparticle preparation, ink formulation with a stable aqueous metal dispersion, and the printed pattern with high electric conductivity. Conduc-

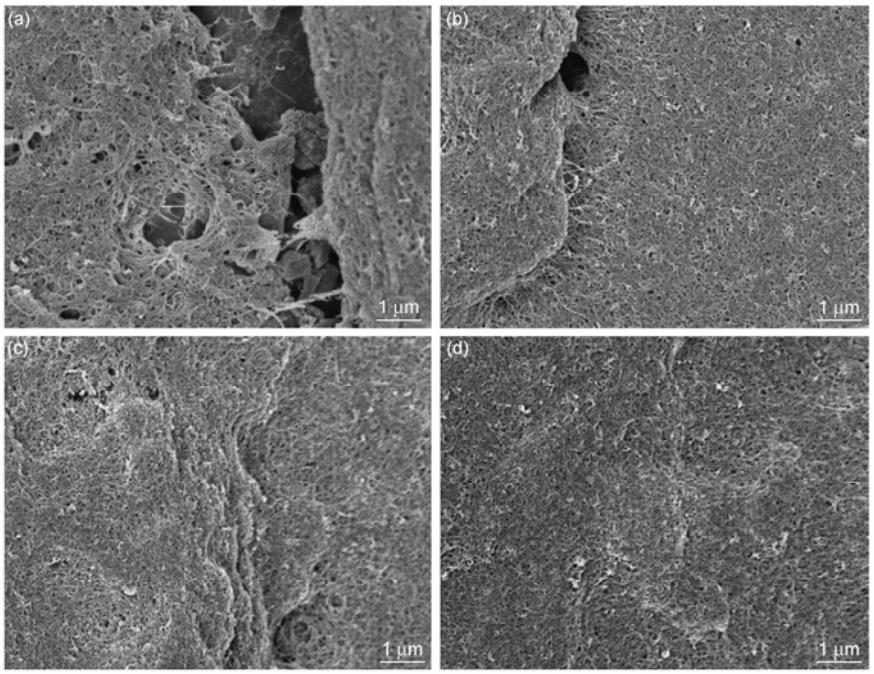

Figure 4 SEM images of carbon stripe on paper (a) one layer; (b) two layers; (c) three layers and (d) four layers [39].

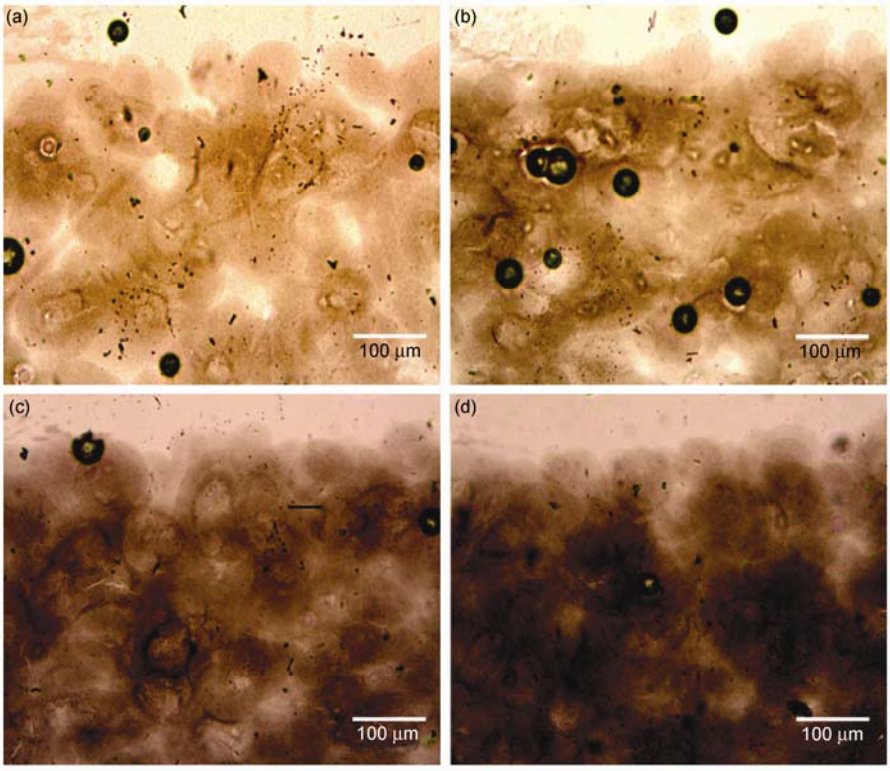

Figure 5 Optical microscope micrographs (printed one layer (a), two layers (b), three layers (c), four layers (d), respectively) [40].

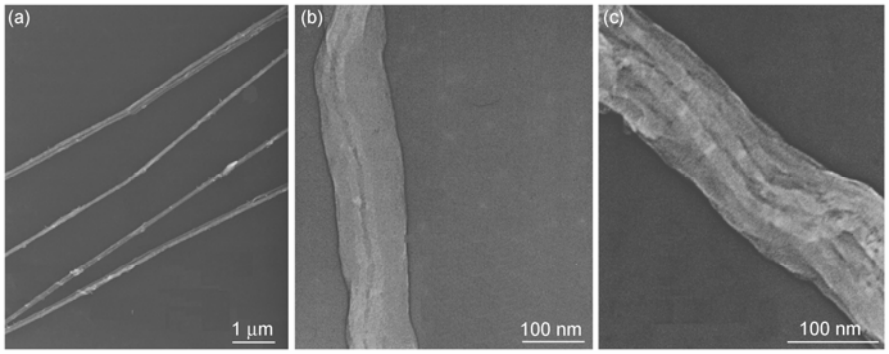

Figure 6 TEM images with different magnifications of nanofibres with well-oriented MWNTs along the axis of nanofibre. (a) TEM image with a low magnification, (b) and (c) TEM images of the composite nanofibres [43].

tive silver inks which exhibit nearly Newtonian rheological behavior has excellent dispersion stability [52]. The viscosity of the silver conductive ink is about 3 mP S at shear rate of 100 s^{-1} and the surface tension is 30–40 mN/m. The sintering temperature monotonously decreases with the decreasing of particle size, which is critical to achieve a high conductivity for flexible electronics. Conductive ink containing nano-sized silver particles with ~20 nm diameter was directly patterned by inkjet printing. After heat-treatment at temperatures of 200°C for 30 min, the printed silver patterns exhibit metal-like appearance and the conductivity.

To prepare silver nanoparticles using the chemical reduction method, stabilizing agents, such as sodium and potassium borohydrides, trisodium citrate, ascorbic acid, hydrocarbons, and gaseous hydrogen, are usually needed to be added as the protecting agent. Poly(N-vinyl-2-pyrrolidone) and thiosalicylic acid are used to protect agent [53,54]. However, the formation of pores caused by the decomposition of the protecting agent during thermal treatment will decrease the conductivity of the silver thin film. To deal with this problem, ink containing a reducing agent (or silver salt) can be jetted onto a receiving substrate containing a silver salt (or reducing agent), and while heating the substrate, a conductive pattern is obtained [53].

Wu et al. [55] adopted ethylene glycol vapor reduction approach to fabricate conductive silver tracks directly from silver nitrate solution by inkjet printing. The silver nitrate precursor can be reduced in ethylene glycol vapor to form

silver at low temperatures. The SEM micrographs of silver array patterns are shown in Figure 7, which are prepared by inkjet printing with different concentrations of silver nitrate solutions and reduced at 250°C for 10 min by ethylene glycol vapor with different frequencies. Analysis results indicate that the silver nitrate has been converted to silver completely. Continuous silver conductive lines with a resistivity of 7.314×10^{-5} Ω cm have been produced, which is relatively close to the resistivity of bulk silver.

Lee et al. [56] demonstrated the possible use of the silver nanocolloid jet generated in the cone-jet mode of electrospray to fabricate functional two-dimensional patterns of silver nanoparticles. Patterns of 100–300 nm in thickness were obtained when the nozzle passed once onto a substrate. The printed spiral inductor produced 9.45 μH and exhibited approximately five times larger resistivity (9.5 μΩ cm) than that of bulk silver after the sintering process. The possibility of using EHD jet printing of silver nanoparticles to obtain conductive line onto circuit boards was also demonstrated [57]. The lines exhibited about three times higher resistivity (4.8 μΩ cm) than that of bulk silver after thermal sintering process. The characteristic impedance of the silver line was about 18 Ω, while the value calculated was 20 Ω.

2.3 Organic materials for ink-jet printing

Organic materials provide a wealth of structural motifs that fuel fundamental investigations in physics, chemistry, and materials. Through careful design and manipulation of a wide range of carbon-based structures, organic/polymer materials are capable of acting as electronic conductors, semiconductors, and insulators [33]. They simultaneously display the physical and chemical properties of organic polymers and the electrical characteristics of metals [58]. All-polymer thin film transistor has been fabricated by high-resolution inkjet printing, shown in Figure 8 [29].

(i) Insulating organic materials. The research of organic dielectric films for inkjet printing has focused on photodefinable gate dielectrics such as polyvinylphenol, polyimide, acryl-based polymer, and sol-gel-derived siloxane-based hybrid polymer. The poly(4-vinylphenol) (PVP) is of particular interest as a low temperature solution-processable dielectric material. Pentacene has continued to be the most widely used small molecule semiconductor primarily due to routinely obtainable thin film transistor hole mobilities in excess of 1 cm^2/V s.

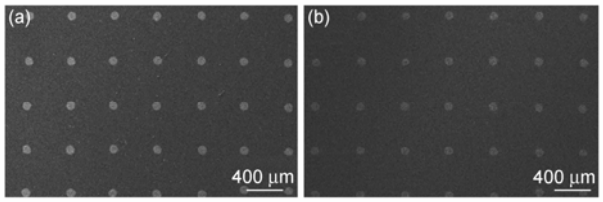

Figure 7 SEM micrographs of silver array patterns. (a) 5 mol/L; (b) 14 mol/L [55].

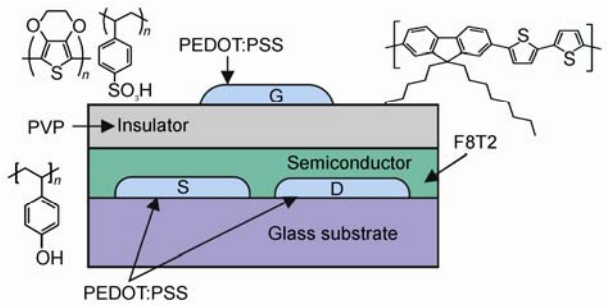

Figure 8 Schematic diagram of the top-gate inkjet printed TFT configuration with an F8T2 semiconducting layer (S, source; D, drain; and G, gate) [29].

PVP is a biocompatible polymer used as a blood plasma expander for trauma victims. PVP is an amorphous polymer possessing high T_g (86°C) due to the presence of the rigid pyrrolidone group, which is known to form various complexes with many inorganic salts [39,59]. Addition of salts with a conducting species such as silver and potassium to PVP has a marked influence on the conductivity of the polymer [40,41]. And the dielectric behavior of PVP doped with ammonium thiocyanate (NH_4SCN) has been studied using dielectric measurements. Choi et al. [60] have used PVP as a dielectric layer instead of SiO_2 gate dielectric in fabricating the inorganic ZnO FETs, and PVP polymer dielectrics exhibits promising electrical properties which operates in the depletion mode with high mobility and high on-current.

(ii) Conductive organic materials. There are several successful conducting polymers, such as Polypyrrole and Poly (3,4-ethylenedioxythiophene) (PEDOT). PEDOT has be studied widely due to its excellent electrical conductivity, such as highly conductive (400–600 S/cm) and electrochemically stable, optoelectronic properties (highly transparent) and thermally stable property (up to 230°C), however, it is insoluble in common solvents which has limited practical applications in inkjet printing [58]. The solubility could be improved by adopting a water-dispersible polyelectrolyte, such as poly-styrene-sulfonate (PSS), as a charge balancing counter ion doping polymerization, which yields poly(3,4-ethylene dioxythiophene)-poly(styrene sulfonate) (PEDOT:PSS) shown in Figure 9 [61].

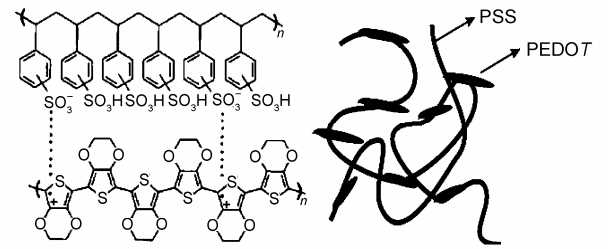

Figure 9 Molecular structure of PEDOT:PSS and schematic structure of PEDOT doped PSS [61].

The resultant PEDOT:PSS is dark blue, electrochemically stable in its p-doped form, moderately transparent with high electrical conductivity (1–10 S/cm). Although PEDOT:PSS has a higher sheet resistance compared to the transparent conductor indium tin oxide (ITO), it is possible to replace ITO. As colloidal dispersions, PEDOT:PSS is stable in water and has excellent capabilities to form films by many methods [62]. Ballarin et al. [63] have compared the continuous film of PEDOT:PSS fabricated by inkjet printing technique with that deposed by spin-coating. No appreciable differences were observed in surface and electrochemical characteristics. These findings show that PEDOT:PSS printed by inkjet printing may be an efficient and clean choice. Eom et al. [64] have printed PEDOT:PSS layer by the inkjet printing technique. Using the newly developed ink formulation of PEDOT:PSS can increase the photovoltaic performance, which results from a reliable print head with optimum wetting, spreading and drying with glycerol and optimized EGBE surfactant. The surface profile images inkjet-printed PEDOT:PSS films without and with additives in different amounts are shown in Figure 10. The conductivity measurements for inkjet-printed PEDOT:PSS films and the current-density versus voltage (*J*-*V*) characteristics of solar cells with different inkjet-printed PEDOT:PSS layers in the dark and under simulated AM1.5 illumination of 100 mW/cm^2 are shown in Figures 11 and 12 separately. We can find that the conductivity of inkjet-printed PEDOT:PSS films are 0.782 S/cm, 152 S/cm, 164 S/cm and 1.28 S/cm from Figure 11.

Hohnholz et al. [65] showed that the effect of additional

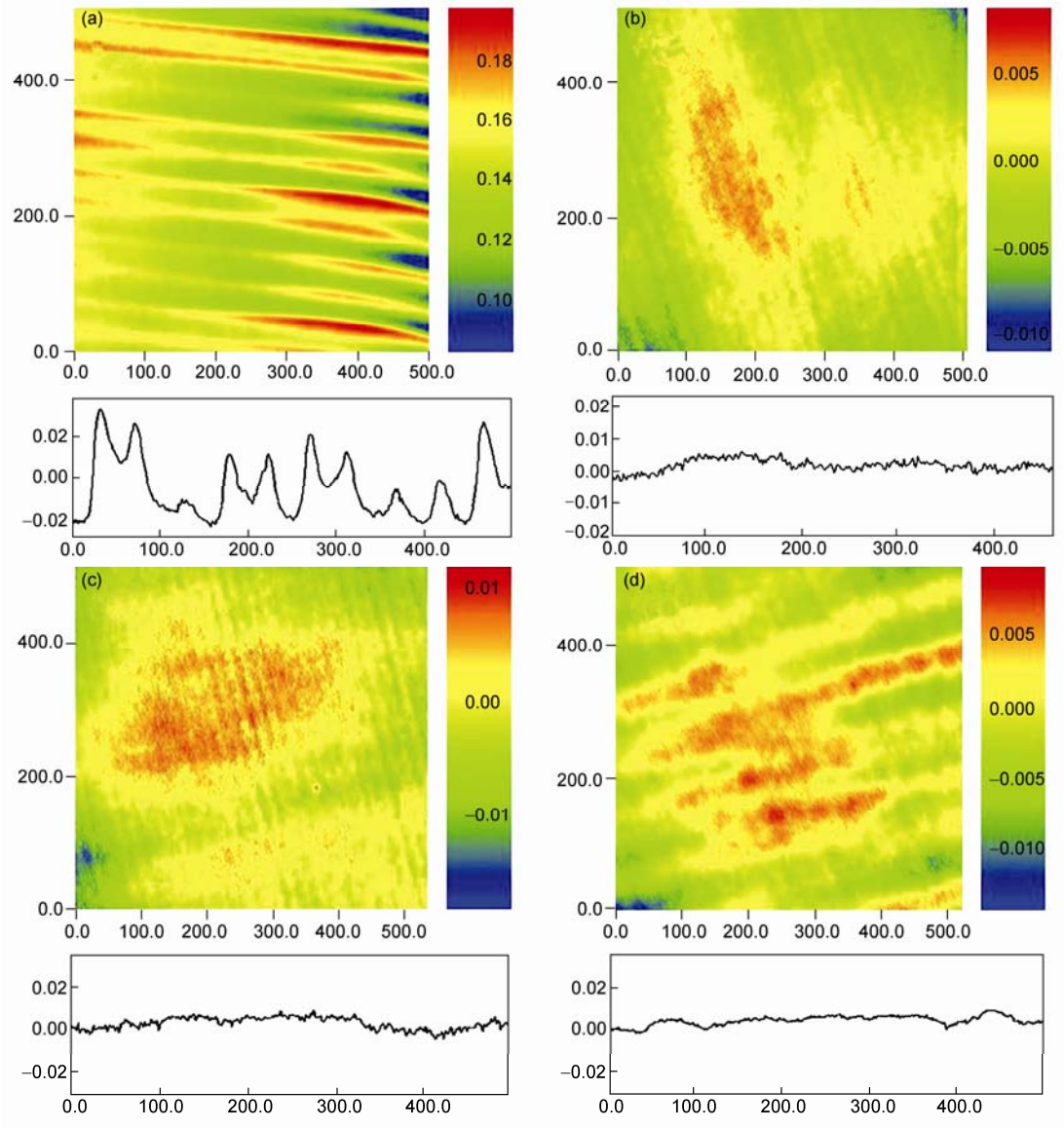

Figure 10 Surface profile images of inkjet-printed PEDOT:PSS films (a) without additives (pure PEDOT:PSS); (b) with 6 wt.% glycerol; (c) with 6 wt.% glycerol and 0.2 wt.% EGBE; (d) 6 wt.% glycerol and 0.4 wt.% EGBE [64].

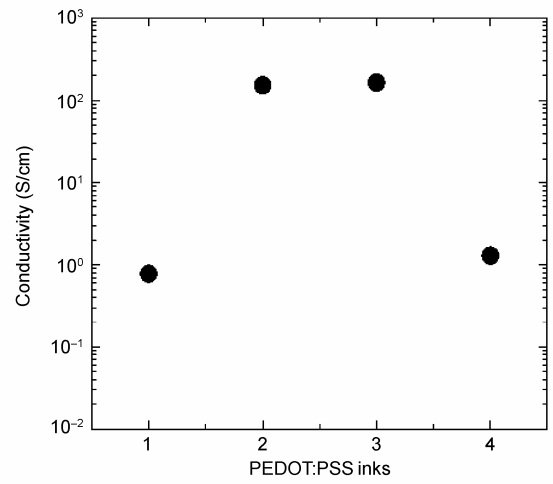

Figure 11 The conductivity measurements for inkjet-printed PEDOT:PSS films: (1) without additives, with (2) 6 wt.% glycerol; (3) 6 wt.% glycerol and 0.2 wt% EGBE; (4) 6 wt.% glycerol and 0.4 wt% EGBE [64].

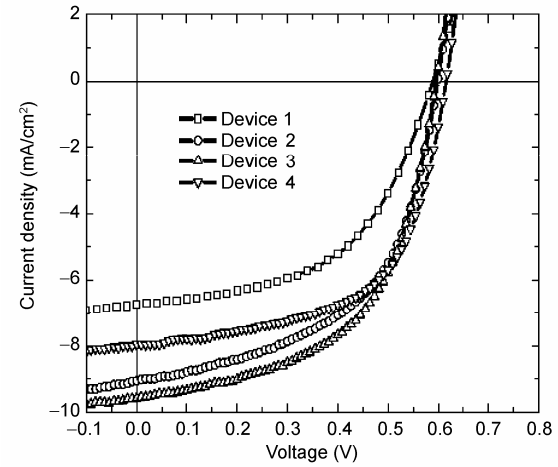

Figure 12 The graph of current-density versus voltage (*J*-*V*) characteristics of solar cell (PEDOT:PSS with (1) without additives, with; (2) 6 wt.% glycerol; (3) 6 wt.% glycerol and 0.2 wt.% EGBE; (4) 6 wt.% glycerol and 0.4 wt.% EGBE) [64].

solvent to improve PEDOT:PSS film conductivity becomes indiscernible and that the overall conductivity is determined by the intrinsic conductivity of the PEDOT as the thickness increases. The thickness of the PEDOT:PSS film showed a linearly increasing tendency as the number of coatings increased. Kwon et al. [66] explained that the resistivity reducing effect originates from the increased PEDOT:PSS film thickness, because the possible numbers of hopping paths for the charge carrier increased as the thickness of the film increased.

2.4 Hybrid/nanocomposite materials

Composites of polymers and carbon nanotubes (P/CNTs) have received considerable research interest because of dramatic improvement of mechanical, thermal, optical and conducting properties, extending their applications in nanoscale devices. P/CNTs can be made with different polymeric matrices including insulating, ferroelectric and conducting etc. The combined synergistic and conducting properties using MWCNTs make them attractive. Jeong et al. [67] formulated functional ink based on thermally crosslinkable organosiloxane-based organic-inorganic hybrid sol-gel materials which are suitable for inkjet printing of dielectric thin films. The inkjet-printed dielectric films exhibited smooth surfaces with the surface roughness of 0.3 nm. It was observed that the leakage current through the printed dielectric is less than 10^{-6} A/cm^2 until a bias of 90 V is applied, and the dielectric constant of printed dielectric is 4.9. In addition, it was confirmed that the inkjet-printed dielectric layer performs electrically similarly to their spin-coated counterparts. However, the residual solvent molecules induce a large hysteresis behavior and positive shift of the threshold voltage for the printed dielectric-based organic transistor.

Dispersion degree strongly influences the rheological properties of nanosized particles containing suspension and, as a consequence, the quality of the deposited film [68]. Furthermore, their applications will be rigorously restricted if the bad dispersion cannot be solved effectively. The measurement results show that mixing with a three-roll mill is an effective tool to break the agglomerates of silver nanoparticles in solvent, resulting in a better dispersion [69]. The dispersion degree effect on the rheological properties and thixotropic characteristics of these suspensions are also elucidated. In addition, the film deposited from suspension with Ag nanoparticles mixed by three-roller mill has the lowest resistivity of approximately 3.64×102 μΩ cm. The use of water as the dispersion medium brings advantages, such as reduced content of volatile organic compounds, which makes the ink environment friendly, nonflammable, and results in complete evaporation of the dispersing medium at low temperature.

3 Processes of inkjet printing

Inkjet printing is familiar as a method of printing text and images onto porous surfaces, enabling rapid prototype production of complex three-dimensional shapes directly from computer software, most recently, direct writing of materials to form electronic, biological, and polymeric devices [26,70,71]. However, its application in flexible electronics results in several challenges in terms of ink formulation, driving mode, substrate selection, and control of solvent evaporation, which do not occur in conventional printing of images. The conventional inkjet printing is "push" processing. Recently, a "pull" processing, named EHD printing, is presented to improve the resolution.

3.1 Conventional inkjet printing techniques

(i) Classes of driving mode. There are two methods most commonly used to generate drops: continuous inkjet (CIJ), in which a continuous stream of drops emerges from the nozzle and uniformly spaced and sized droplets are obtained by imposing a periodic perturbation, or DOD, in which drops are ejected as needed. Its development path and technology map have been discussed in detail [71]. The most important properties are surface tension and viscosity of ink, and the frequency and amplitude of the modulation. Generally, CIJ systems operate with fluids of lower viscosity than DOD, and at a higher drop velocity, and tend to require larger quantities of fluid for pumping and recirculation. DOD is widely adopted due to its high placement accuracy, controllability, and efficient materials usage.

DOD uses pulses, generated either thermally or piezoelectrically (Figure 13) [71], thermal buckling [30] and acoustic [72], to push the solution droplets. In thermal bubble (Figure 13(a)), a thin layer of liquid is heated locally by a thin film heater in a few microseconds to form a rapidly expanding vapor bubble that ejects an ink droplet. The initial actuation pressure is close to the saturated vapor pressure of the liquid at the superheat limit (about 4 MPa for water, and 1 MPa for organic solvents). The minimum printable droplet size of a thermal bubble inkjet device is then about 0.5 μm for water and 1 μm for methanol and toluene [30]. The temperature raises to about 300°C, so a main problem is to avoid clogging of the nozzle [27]. It is not suitable for polymers printing [37]. Piezoelectric inkjet printing (Figure 13(b)) relies on the mechanical action of a piezoelectric membrane to generate a pulse [37]. Nozzle sizes are in the range of 20–30 μm, and droplets are in the range of 10–20 pL [27]. The diameter of an ink drop on a substrate is about twice the size of the released drops.

To maintain high printing throughput, a bigger and denser inkjet array has to be formed. Printheads typically contain tens, hundreds or even thousands of separate nozzles, fed by a single ink manifold but each individually addressable [70]. Bulk piezoelectric material used in the printheads lead to a large device area to achieve enough actuation strength, so the number of devices on a printhead is limited [30]. Thermal buckling means are also not practical for the same reason. Thermal bubble inkjet devices only need a small thermal heater for actuation thanks to the free expansion of the vapor bubble. They are compatible with micro-fabrication, which makes a large inkjet array feasible [30]. Wang et al. [73] developed a print head using a dense array of thermal bubble inkjet devices. Experimental results show that this print head is capable of generating water droplets as small as 3 μm in diameter.

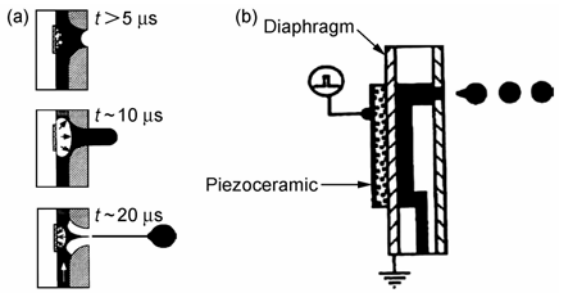

Figure 13 Schematic representation of inkjet printer head. (a) Thermal; (b) piezoceramic [71].

(ii) Physical and chemical mechanism of drop formation. The applications in printable electronics require higher print rates, better resolution and higher reliability while printing more complex, non-Newtonian and heavily solids-loaded liquids, which makes the understanding of the physics involved in the precise manipulation of liquid jets and drops ever more important. The main stages of DOD drop formation, including ejection and stretching of liquid, pinch-off of liquid thread from the nozzle, contraction of liquid thread, breakup of liquid thread into primary drop and satellites, and recombination of primary drop and satellites, are being analyzed based on the theoretical and experimental results [74]. The proper understanding and control of jet formation and subsequent motion of the jetted materials requires physical studies into material properties at very high shear rates, instabilities of jets, drop formation and motion, stretching of fluid ligaments and the aerodynamic and electrostatic interaction of jets and drops in flight [75]. Numerical simulations have been carried out based on one-dimensional models and two-dimensional axisymmetric Navier-Stokes equations. Experimental observations of the dynamics at the micron scale have compared with the simulated flows [74].

The transient liquid velocity distribution causes liquid surface deformation at the nozzle forming a thin neck, then droplet detaches if the liquid neck is sufficiently small. The dominant forces which control the behavior of liquid jets and drops arise from inertia, viscosity and surface tension. As a droplet is expelled, energy goes into viscous flow, surface tension of the drop, and kinetic energy. In addition to the main drop a smaller satellite drop is created slightly later which recombines with the main drop in front of it after a few periods. The formation of secondary satellite droplets should be suppressed [37]. The linear analysis of Rayleigh does not predict the formation of satellites at all [36]. For a given ink, satellite formation is normally controlled pragmatically by changing the amplitude of the driving disturbance.

Usually, smaller nozzles allow smaller droplets and higher resolution. However, as nozzle size decreases, surface tension and viscosity force will increase, and a higher actuation pressure is necessary to accelerate the liquid. A major concern in ink design is the “first drop problem” which is the clogging of nozzles by partly dried ink [27], so DOD system is the need for the ink to dry or solidify on the printed surface but the nozzle. This can be addressed at the printhead, by appropriate cleaning and capping for example,

and at the substrate by using low volatility inks and absorbing substrates, heaters, dryers or UV-curable inks [36]. The chemical and physical compatibility of head, ink and substrate is still unclear.

(iii) Control of morphology, feature sizes and performance. Recent advances in the performance of OTFTs are largely due to fine control of the morphology and the resolution in semiconductor thin films in addition to the development of active organic materials. The patterns range from simple island areas to lines over large distances, even to large area. Further, as drops are added to the printed liquid line, instabilities, such as necks, may form due to the dynamics of the spreading and drying of the printed liquid line [76]. It is a challenge to print lines over long distances, control of feature sizes and morphology.

Charge-carrier transport in TFTs is governed by their morphologies. Fine morphology benefits to print pinhole-free layers to avoid opens or shorting of devices. The morphology can be achieved by adjusting the deposition conditions such as surface treatment of the substrate, modifying solvent properties, and adopting organic semiconductor materials with strong intermolecular p-p interactions [77]. The fluid dynamics involved in drop formation, wetting and spreading play an important role in defining the surface roughness and decreasing the feature size. These low viscosity fluids are capable of flowing through the nozzle without clogging and forming consistent drops that solidify by liquid evaporation, however, dimensional control of the feature can be a major problem. Therefore control of ink spread on the substrate is crucial [78].

The spreading of solution can be reduced by prepatterning the surface with different regions of differing wettability [79] or surface topography [80] on the substrate, formed by photolithographic or other means. Small gaps can be created using a self-aligned printing method that relies on differences in wettability [81]. The use of extra patterning steps are adopted in the process with extra processing equipment. This strategy enables inkjet printing of all-polymer TFTs with channel lengths in the micrometer range (Figure 14) [29], where (a) is the schematic diagram of high-resolution inkjet printing onto a prepatterned substrate, (b) is AFM showing accurate alignment of inkjet-printed PEDOT:PSS source and drain electrodes separated by a repelling polyimide line with 5 μm, (c) shows F8T2 semiconducting layer and PEDOT:PSS electrodes, and (d) is optical micrograph of the device. Through appropriate control of the printing process, Bao [82] demonstrate the transistors with channels as short as 250 nm. Sele et al. [83] have demonstrated a self-aligned printing technique with standard inkjet-printing equipment, but is capable of achieving sub-100 nm resolution without any lithographic step. A combination of inkjet and laser ablation/sintering has been used to fabricate a variety of passive and active components of and on polymers [84].

When the liquid drop is ejected from the printhead, it takes a ballistic trajectory and lands on a certain position on a substrate. Usually, the expected error in the ejected drop placement is about 5–10 μm [1]. However, what matters in practice is the accuracy with which a droplet can be deposited on a surface. The drop placement accuracy does not only depend on printhead positioning accuracy, but also on

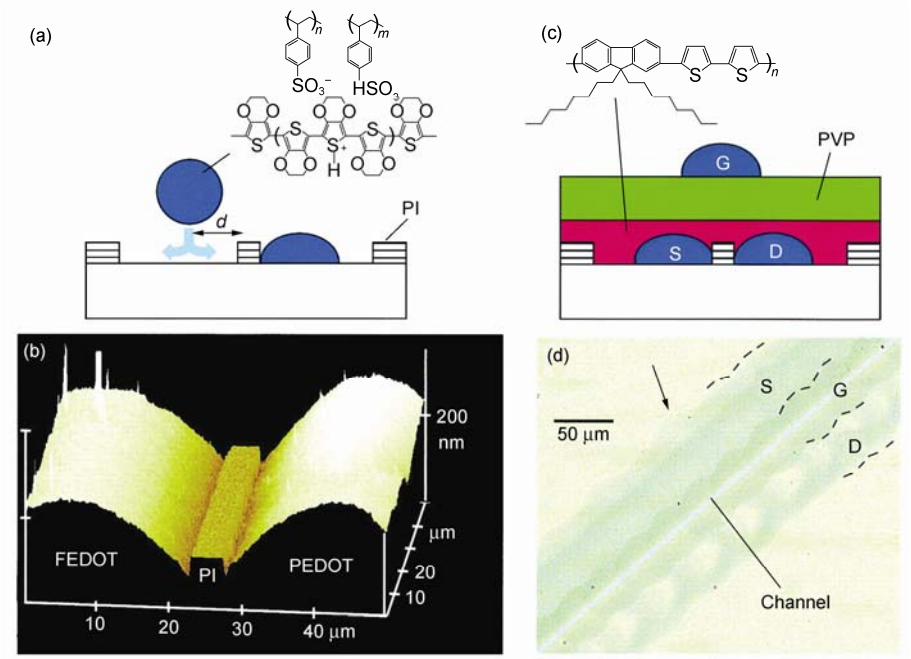

Figure 14 Schematic diagram of a top-gate inkjet printed TFT (S, source; D, drain; and G, gate) [29]. (a) Schematic diagram of high-resolution IJP onto a prepatterned substrate; (b) AFM showing accurate alignment of inkjet-printed PEDOT/PSS source and drain electrodes separated by a repelling polyimide (PI) line with L= 5 μm; (c) schematic diagram of the top-gate IJP TFT configuration; (d) optical micrograph of an IJP TFT (L = 5 μm).

the angle of the printhead relative to the substrate. Strong side wind can also deflect droplets. Minimizing the distance between the printhead and the substrate can reduce the impact of both. Moreover, it is important that the ink wets the nozzle uniformly, otherwise the drop goes off at an angle [37].

3.2 Electrohydrodynamic printing techniques

In recent years, there are considerable interests in developing new printing technology for patterning materials in nano-scale. EHD printing pulls the fluids rather than pushes them like conventional inkjet printing. EHD printing, in which electric fields are employed instead of thermal bubble, piezoelectric and acoustic wave, uses a fine jet generated at the apex of a liquid cone in the cone-jet mode to create spray by electrospraying (Figure 19), fibre by electrospinning (Figure 21) or droplets by EHD jetting (Figure 24), respectively [56]. There are some unique features for EHD printing, such as allowing submicron resolution [85], and particulate or polymer solutions can be easily emitting without clogging the nozzle. This also means that the resolution is not limited by the nozzle diameter [78]. Using coarser nozzles prevents them from clogging, but at the same time, the droplets can be of sub-micrometer size [86]. EHD printing has great potential to offer complex and high-resolution printing and is opening new routes to nanotechnology.

(i) Mechanism of EHD printing. Three types of EHD printing hold the same mechanism of electrohydrodynamics and the homologous experiment setups [78,87]. It is promising for all the three methods used in flexible electronics, such as electrospray for thin film layer, electrospinning for interconnection, and EHD inkjet for electrode. The charged liquid is ejected from the nozzle when the electrical force locally overcomes the liquid surface tension. The liquid at the outlet of a nozzle is subjected to an electrical shear stress by maintaining the nozzle at high electric potential. This non-mechanical, electrostatic technique use an electric field to draw out a liquid from a nozzle to form a Taylor cone which then breaks up into a stream of very small droplets [88]. Figure 15 shows schematics of this method employed to produce drops. There are other various printing modes with various jet structures and break-up mechanisms, depending on the flow rates, the applied voltages, liquid properties, and nozzle configurations [89].

Patterns using EHD printing have been fabricated by the continuous cone-jet mode [56] and the pulsating jet mode [90]. The continuous cone-jet only form continuous lines and not a series of dots. The pulsating jet mode has been reported to produce discontinuous lines or a series of dots in a DOD fashion by use of the pulsed voltage [91] or lower DC voltage than that for the continuous cone-jet mode. However, as pulsed voltage frequency increases, drops may not generate at every pulse although the meniscus oscillates or it may break up into many droplets [87]. The liquid flowing out of a capillary nozzle, which is maintained at high electric potential, is forced by the electric field to be dispersed into fine droplets.

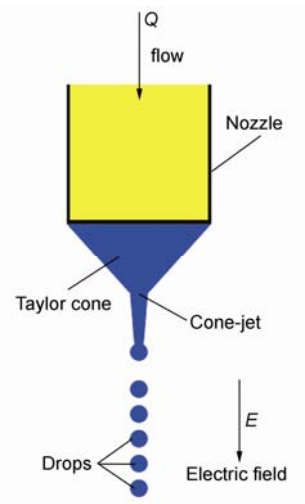

Figure 15 Production of drops through EHD tip streaming [88].

EHD printing comprises four component: a reservoir (or a syringe pump), a needle with coated metal, and a high voltage generator and a collective electrode [78,92]. In the experimental setups, the differences between them are the solution properties, the distance and voltage between needle and collector. The discharge needle serves as an electrode and is made of stainless steel. The second electrode, which may be a pin, a ring or a plate, is placed directly below the needle and is grounded. It has been proved that the sol-gel solution can be ejected through the needle and controlled by the movement of the syringe piston. The electric field established between the two electrodes breaks the emerging fluid jet into droplets or fibre [78].

The droplets of liquid acquire stable shapes when they are subjected to a high electrical potential difference, since the shapes are a balance of gravity force F_g, surface tension force F_{st} and electric field force F_e as shown in Figure 16 [93]. If the potential is not too high, the droplets surface experiences a considerably electrostatic pull. The surface deformation is further triggered and the electric field result

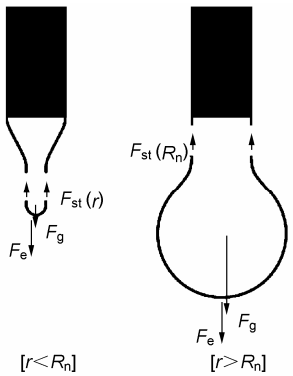

Figure 16 Schematic of liquid meniscus at the nozzle tip [93].

in charge concentration that will start to form a liquid cone called Taylor cone. When the critical potential reached, the balance of electric forces and surface tension was destroyed. A high speed thin jet emanates from the apex of the cone as shown in Figure 17 [94] which show drop in electrical field by the time and voltage varying. Through adjusting different parameters for different solution, the three types of EHD printing can be realized, whose differences are illustrated in Table 3.

The jetting modes of dripping, microdripping, and cone-jet are observed as shown in Figure 18 [86] by varying the applied voltage as well as the flow rate. The dripping mode represents jetting drop by drop after the swelling on the nozzle tip in the absence of an electric field. The curved liquid meniscus at the nozzle tip is not swollen to a spherical shape but is formed into the shape of a cone. A monodisperse droplet is formed directly at the meniscus apex in the microdripping mode [93]. In the cone-jet mode, the cone is extended by a jet that breaks up ink into very tiny droplets. There is no study on the variation of drop generation frequency in the pulsed cone-jet mode patterning. In addition, any visual results to control the drop size and the spacing in the pulsed cone-jet mode patterning have not been reported [87].

In order to estimate the droplet radius r of the ink that is ejected by the electrostatic force through the nozzle, the balanced force equation is adopted [93]:

$$F_{\mathrm{g}} - F_{\mathrm{st}} + F_{\mathrm{e}} = 0. \quad (2)$$

The trial and error method was used to calculate r in the balanced state of the three forces, which show r is the variable for all the three forces. Meanwhile, the three forces are also affected by the droplet radius [86,93].

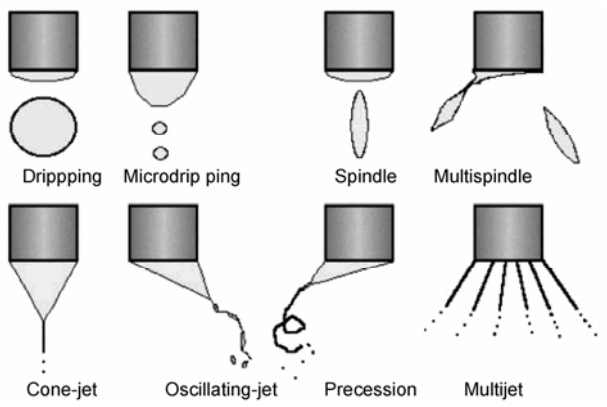

Figure 18 Various modes of electrohydrodynamics [86].

(ii) Electrospraying. Electrospraying (EHD spraying), shown in Figure 19, utilizes electrical field for liquid atomization. The solution is usually a sol-gel solution containing nano-particulates with a higher viscosity than ink used in conventional inkjet systems [78]. It can be adopted to handle particulate solutions, such as depositing thin and thick films of PZT [95] and gold [78] using sol-gel precursors. Its advantage includes [86,96]: (1) Droplets can be extremely small, even down to 10's nanometers; (2) The charge and size of the droplets can be controlled to some

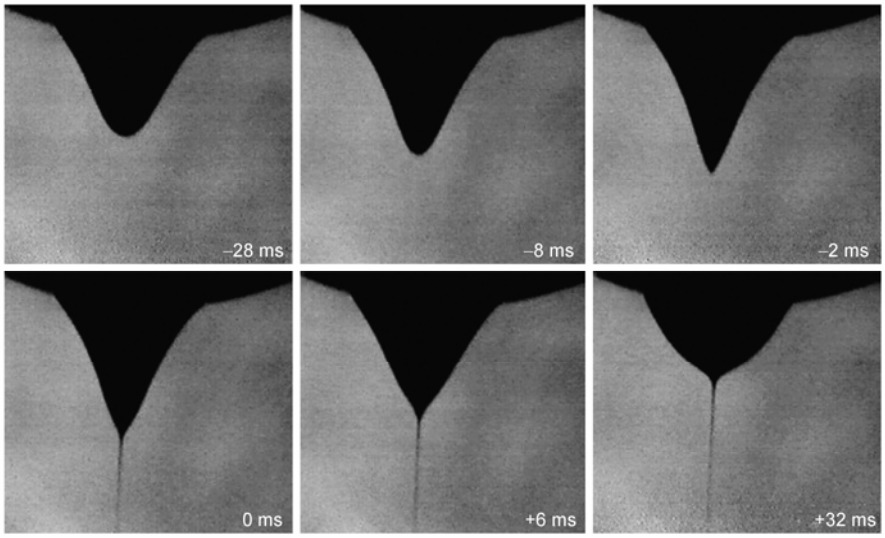

Figure 17 The evolution of the shape of a liquid [94].

Table 3 Comparison of the three EHD printing methods

E-Printing	Mode	Voltage	Electrode distance	Solute	Pattern
E-jetting	Cone-jet, Microdripping	0.5–3 kV	0.1–1 mm	Polymer, nanoparticle	Dot, discrete line
E-spinning	Cone-jet, Multi-jet	1–10 kV	10–50 mm	Polmer, nanomaterials,	Continuous; ine (fibre)
E-spraying	Cone-jet, Multi-jet	15–30 kV	100–250 mm	Almost materials	Thin film

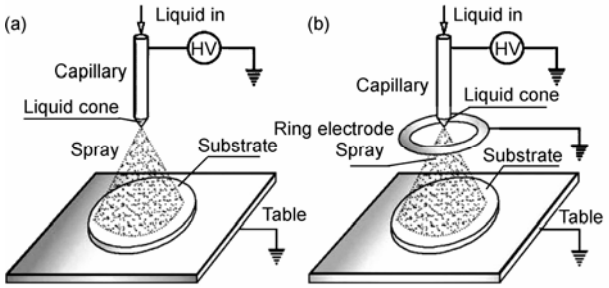

Figure 19 Schematic illustration of an electrospray printer [96]. (a) Simple nozzle; (b) nozzle-extractor system.

extent by adjusting the flow rate and voltage applied to the nozzle; (3) The size distribution of the droplets can be nearly monodisperse. In electrospraying, particles with the same size hold the similar thermodynamic states, which offers significant advantages in building more uniform film than those obtained via other methods and reducing the number and size of voids and cracks in flexible electronics [86]. This method has been employed to produce organic films, at the present time, the thinnest film reported is 15 nm [97]. It also can be adopted as direct writing technology as shown in Figure 20 [86]. Recent advancements in nano-electrospray technologies have been briefly reviewed by Salata [98]. A comparison between spray forming technology and conventional casting was performed by Yu et al. [99]. The electrospray methods used for thin-film deposition have been reviewed by Jaworek [96]. The applications of electrospray are particularly discussed by Chen et al. [100], especially for microelectronics and biology.

Motion of the charged droplets can be controlled by an electric field. The deposition efficiency of the charged spray on an object is usually higher than that for uncharged droplets [86,96]. Although, there are many spraying modes, electrospray deposition is usually studied in two modes defined in Figure 19 [96], simple nozzle for direct spraying and nozzle-extractor system. The difference is that an extractor electrode insert in the space between capillary and substrate. That can avoided uneven film that attributed to the damage of substrate, but some drop could fall on to the extractor electrode. Figure 19(a) is that only fragments of liquid are ejected directly from the meniscus at the capillary outlet. These fragments can be in the form of regular large drops, fine droplets, or elongated spindles at the moment of their detachment. In Figure 19(b), the liquid is elongated into a fine jet, which disintegrates into droplets due to its instability. It was observed that the jet could be smooth and stable or could move in a regular way: rotate around the capillary axis or oscillate in its plane.

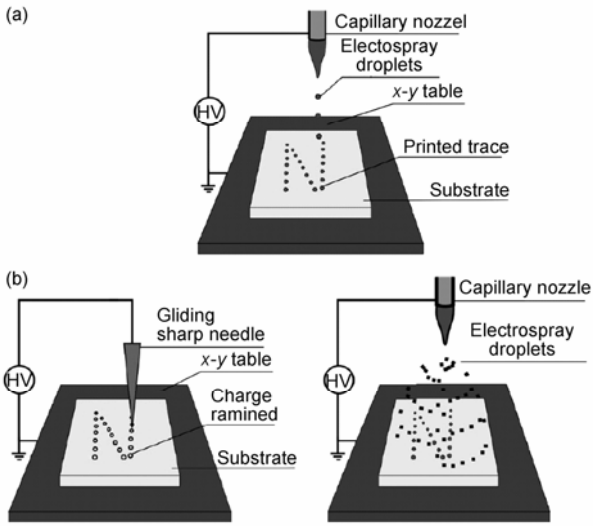

Figure 20 Schematic of direct writing: (a) One-step process using electrospray droplets and (b) two-step process: ion deposition with a sharp needle followed by nanoelectrospray [86].

Fujihara et al. [101] fabricated a large-area TiO_2 electrode layer using electrospun nanorods for dye-sensitized solar cells. They first get TiO_2 nanofibres by electrospinning, then obtained electrodes by mechanical grinding of these fibres. These rods were dispersed in an aqueous $TiCl_4$ which can supply a better connectivity of rods. After electrospray deposition of this solution, the film was sintered. Through these methods, it supplies a uniform large-area (20 cm^2) electrode with thin film and an industrial apparatus. Cich et al. [102] produced a plasma display active layer on Si(111) substrate. The spraying process took place in an atmosphere of nitrogen and ethanol. The morphology of the layer and photoluminescence intensity were found to be dependent on the deposition parameters such as voltage, flow rate, and so on.

(iii) Electrospinning. Although the term "electrospinning" (EHD spinning) was used around mid-1990s, its fundamental idea dates back more than 60 years earlier. It is a pity its understanding is still very limited [103]. A typical electrospinning set-up is shown in Figure 21 [92]. It has been recognized as an efficient technique for the fabrication of polymer nanofibers from the submicron diameter down to the nanometre diameter. Although there are other methods of fabricating nanofibres such as phase separation, tem-

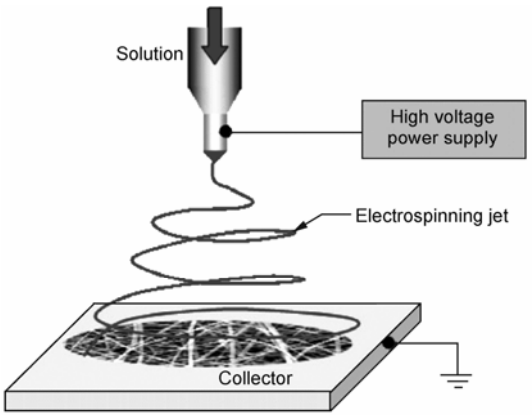

Figure 21 Schematic illustration of an electrospinning printer [92].

plate synthesis, drawing, self-assembly [92,103], few, if any, can match electrospinning in terms of its versatility, flexibility and ease of fibre production. Various polymers have been successfully electrospun into ultrafine fibers [103]. Theoretically, the emitting to form the fibre will continue as long as there is enough solution to feed the electrospinning jet. Fabrication of nanofibers of conductive polymers has recently been demonstrated in the design and construction of micro- and nanodevices [104,105].

A high voltage is used to create an electrically charged jet of polymer solution or melt out of the pipette. Before reaching the conducting collector, the solution jet evaporates or solidifies, and is collected as an interconnected web of small fibers [103]. In addition, there are two other emerging types: Non-spinnerets apparatus explored by Yarin et al. [106], and near-field electrospinning developed by Sun et al. [105] and Hellmann et al. [107]. The recent progress in electrospun nanofibers was summarized by Fang et al. [108] with an emphasis on their applications. So far, nearly one hundred different materials have been successfully spun into ultrafine fibers [103]. Most of them are polymers, inorganic materials, and compound with nanomaterials (nanotube, nanoparticle).

Although the jet is stable near the tip of the spinneret, the thin jet from the apex of the cone is accelerated toward the collector, in the flight, solidifies into a fiber as the solvent evaporates. Unfortunately, the jet will often exhibit complex dynamics, such as the 'whipping' instability that causes the jet to dance around after a short distance from the tip. As shown in Figure 22 [94], there are several kinds of instabilities in normal situation, so the controllability of the electrospinning process is critical. There are two kinds of works toward the instabilities: (1) limited works toward the control of electrospinning [105], including aligning nanofibers by electrical field and using rotational mechanical mandrels; and (2) numerous investigations toward the fundamental physics and chemistry of electrospinning [103], including the effects of polymer solution concentration, applied voltage, and electrode-to-collector distance.

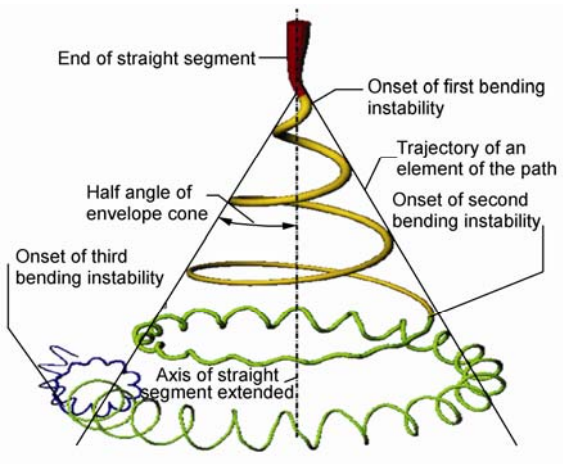

Figure 22 Evolution of the shape of a liquid drop in electrical field by the time and voltage varying [94].

MacDiarmid [104] presented a Nobel lecture: "Synthetic Metals: a novel role for organic polymers", gave an insight into the application of flexible electronics, and made the first conducting polymer fiber (diameter 950 nm to 2100 nm). Although the fibre is thick, the attempt is rousing. Chronakis et al. [58] fabricated the conductive polypyrrole nanofiber with diameters in the range of 70–300 nm. Jeong et al. [109] fabricated MWCNT/nylon composite nanofibers and tested their I-V performance. Zhang et al. [43] also spinned nanofibres with diameter with ~100 nm and aligned across the gap between the parallel electrodes.

Sun et al. [105] developed a near-field electrospinning (NFES) to deposit solid nanofibers in a direct, continuous, and controllable manner. Figure 23(a) illustrates the schematic setup that merges several disparate concepts, including the electrode-to-collector distance h in the range of 500 μm to 3 mm, the liquid polymer solution supplied in a manner analogous to dip-pen, a solid tungsten spinneret of 25 μm tip diameter as illustrated in Figure 23(b), the applied electrostatic voltage reduced due to the short electrode-to-collector distance. Figure 23(c) shows that a droplet of 50 μm in diameter is extracted from the polymer solution. A Taylor cone is observed in Figure 23(d). As the process proceeds, the polymer solution on the tungsten tip is consumed and its diameter shrinks, leading to a smaller Taylor cone and thinner nanofibers as observed in Figure 23(e). NFES combines dip-pen, inkjet, and electrospinning by providing the feasibility of controllable electrospinning for sub-100-nm nanofabrication.

(iv) Electrohydrodynamic jetting. EHD jetting is a DOD control of a droplet in microdripping mode, which can deliver highly uniform droplets and can pattern any geometry. It has been paid more attentions in the high resolution patterns, since it can directly form micro/nano-scale patterns with different materials, ranging from insulating and conducting polymers, from solution suspension to SWCNs. Many experiments were carried out by varying the bias and pulse voltages to implement the DOD operation of jetting droplets and to investigate the optimal pulse conditions for jetting [93]. However, there has been little in-depth study of EHD jetting.

Figure 24 shows a schematic diagram of the EHD jetting system [85], where Figure 24(a) is SEM images of a microcapillary nozzle, Figure 24(b) is nozzle and substrate configuration for printing, and Figure 24(c) is the whole printer set-up. A jet is emitted through the tip of needle and controlled by the movement of the table. The droplets are deposited on the substrate placed on the second electrode. The internal diameter of the needle or nozzle usually is about 0.1–1 mm. If the nozzle can be fabricated with smaller internal diameters, higher resolution can be patterned. EHD jetting can produce droplets at least an order of magnitude smaller than the nozzle size [85]. The droplets can be of

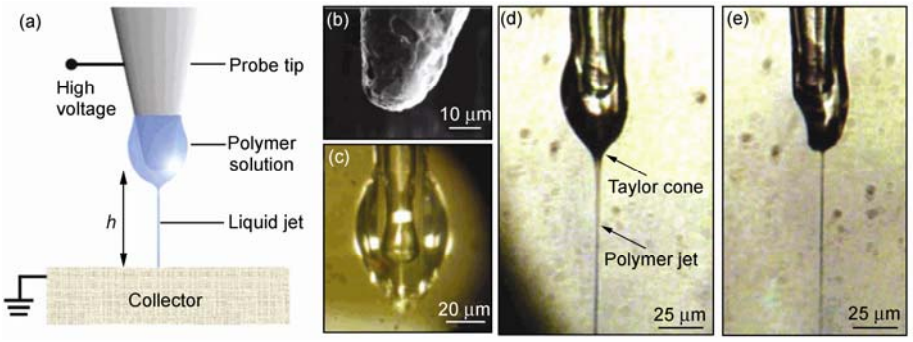

Figure 23 Schematic representation of NFES processing [105]. (a) Schematic representation of NFES; (b) SEM photomicrograph showing the nozzel; (c) an optical photo showing a 50 μm diameter polymer solution droplet; (d) a polymer jet is ejected from the apex of a Taylor cone under applied electrical field and observed under an optical microscope; (e) the size of the polymer droplet decreases as the polymer jet continues to electrospin.

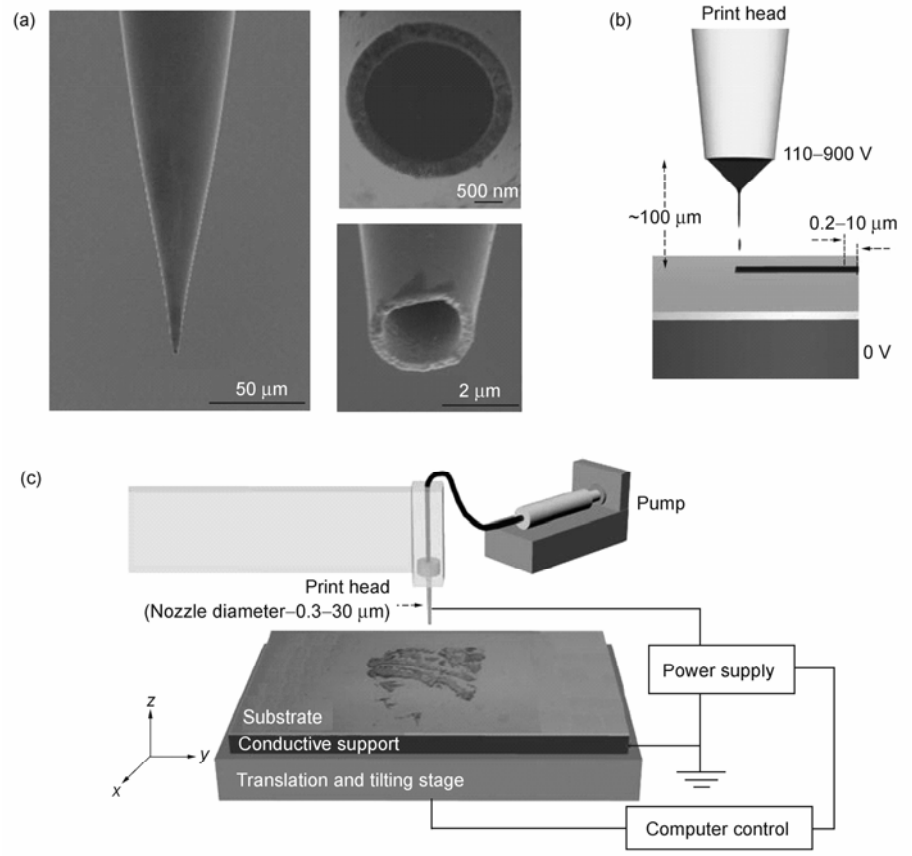

Figure 24 Nozzle structures and schematic diagrams of a high-resolution e-jet printer [85]. (a) SEM images of a gold-coated glass microcapillary nozzle (2 μm internal diameter); (b) nozzle and substrate configuration for printing; (c) printer set-up.

micrometer size even nanometers.

Rogers et al. [85] described the use of electrohydrodynamically induced fluid flows through fine microcapillary nozzles for jet printing of patterns and functional devices with submicrometre resolution. High-resolution printed metal electrodes, interconnections and probing pads for representative circuit patterns and functional transistors with critical dimensions as small as 1 μm demonstrate potential applications in printed electronics. They patterned Au electrode lines ~2 μm width after etching and stripping. An array of source/drain electrode pairs is separated by ~1 μm. Another interesting work is that they used SWNTs as semiconductor connecting the printed electrode pair to construct a TFT, whose performance is much better. If patterns of continuous lines use the 2 μm internal diameter nozzle and a printing speed of 10 μm/s, the line width are ~3 μm. If an 1 μm internal diameter nozzle is adopted, line widths are about 700 nm.

Sekitani et al. [110] adopted the similar system to build OTFT whose accuracy reaches sub-femtoliter. They defined metal contacts with 1 μm resolution on the surface of high-mobility organic semiconductors to create p- and n-channel transistors. The transistor employ an ultra-thin low-temperature gate dielectric based on a self-assembled monolayer that allows transistors operating with very low voltages. The ink consists of monodispersed Ag nanoparticle with a diameter of 2–3 nm in tetradecane. Sub-femtoliter printing significantly reduces the calcinations temperature, which means the damage of organic semiconductor can be avoided. The nozzle of the sub-femtoliter inkjet system is fabricated from a very fine capillary glass tube with a tip diameter of <1 μm. The inside of the capillary tube is hydrophilic, whereas the outside of the tube is hydrophobic.

Lee et al. [56] formed conductive silver line and test its electrical characterization. He used a nozzle (180 μm) much larger than a conventional inkjet nozzle (about 20 μm), and a micronsized jet can be generated. Choi et al. [111] studied the jet diameter relationship with nozzle size and electric field in jet pulsations. They observed that the fundamental pulsation frequency is proportional to the electric field strength. Choi et al. [93] tested jetting performance for various bias voltages and pulse signals to find the optimal jetting conditions. To increase output and stabilize the cone-jet mode, Lee et al. [112] developed an EHD jetting that uses an addressable multi-nozzle fabricated from a silicon wafer to reduce the interference and distortion in the electric field.

(v) Control of EHD printing process. EHD printing is a very complex process, whose microstructure and morphology subjected to two groups of factors [85,86,92,98,103,105,113], material factors including the structure of materials (molecular weight, type of molecular chain, chain length) and the physical properties of solution (viscosity, Young's module, conductivity, permittivity), and manufacturing factors including the controllable parameters (needle-to-collector distance, voltage, diameter of nozzle) and the circumstance parameters (pressure, humidity, temperature). Flexible electronic devices are usually fabricated with various materials which are dissolved in solvent and dispersed into a colloidal state. To obtain a stable jet, the above factors have to be controlled [78].

There is a challenge to control the orientation of jet/drop/fibre. Usually, the dynamic behavior is very complex because of the disturbance by repulsion of charges and air perturbation. There are differences between jet/drop and fibre in manipulating the orientation. In EHD jetting and electrospraying, the last phase of jet or drop is liquid when they fly down to the substrate. Although a single drop is controlled in EHD jetting and many droplets are controlled in electrospraying, EHD jetting is more complex because EHD jetting forms certain patterns but electrospraying forms thin film. Jaworek et al. [96] used a guard electrode to acquire more uniform electric field in the space to improve operational properties of electrospray. Kim et al. [114] applied a pyrex guide tube focused the droplets on the substrate surface. The film obtained was more uniform by the heated sheath gas pumped through the tube. Sorensen et al. [115] designed a 'trumpet-ended' nozzle made of stainless steel capillary with central sharp electrode. In EHD jetting system, two kinds of methods are adopted, reducing the needle-to-collector distance and the diameter of needle, and designing some new nozzle that can avoid the instability in jet broken [93,112].

However, in electrospinning, the last phase of jet is solid when they fly down to the substrate. In flight, the control aim is to get certain orientation or an electrospun nanofibre assembly with collector. There are three types of control methods: (1) dynamic mechanical device [92]: there are many types of dynamic mechanical devices that are used to collect nanofibre, including drum, static plane, and added drawing. (2) Manipulation of electric field [92]: many auxiliary electrodes were applied with different shape and position. (3) Near-field manipulation [105]: the jet is control by reducing the distance of two electrodes, meanwhile the voltage is also decreased.

The breakup process should be controlled for its proper application according to the desired linewidth of the pattern in EHD printing [56]. In summary, there are some important relations that had been investigated. (1) When a higher molecular weight is dissolved, the viscosity of the solution will increase. Some certain viscosity is necessary for forming continuous nanofibre, but detrimental for drop broken in electrospraying and EHD jetting. (2) Surface tension has the effect of decreasing the surface area per unit mass of a fluid. It is useful for small drop formation in EHD jetting and electrospraying. However, it will result in beads generation in electrospinning. (3) When the conductivity of the solution is increased, the jet velocity will be much faster and the stretching force is enhanced, which result in droplet and fibre with smaller diameter. (4) Permittivity directly affects the surface charge density. In electrospinning, it will increase the "whiping", so the fibre diameter was relatively reduced, but it is hard for orientation. In EHD jetting and electrospraying, that will decrease the drop and increase the instability. (5) High flow rate of the solution through the needle will increase the diameter of jet [94]. A general law can be formulated that the deposition rate of a layer is proportional to the final thickness of the layer [86]. (6) Temperature is a parameter with pressure and viscosity. In detail, higher temperature can increase evaporation rate and decreasing viscosity. (7) Nozzle with smaller diameter can attain higher resolution. (8) The distance affects flight time and electrical field. Larger distance will create small drop and fibre, but also large instability. (9) The electric field is a complex parameter for reducing droplet size [94] and has influence on morphology of drop and fibre, the resolution and stability. The film thickness, its crystallinity, texture, and deposition rate can be easily controlled by varying the voltage, flow rate, concentration of the material to be deposited, and the substrate temperature [86]. For example, to

obtain a stable jet, the growth rate of the jet should be decreased by applying high axial electric fields. However, it can not only increase the axial components of the electric fields but also increase the radial components. Increasing the radial components might amplify the growth rate of the jet. Lee et al. [56] found that the pin-type ground electrode with a 400 nm diameter effectively increased the axial electric fields but did not greatly change the radial electric fields, so the jet breakup was reduced. Additionally, the guide ring with an inner hole reduced the chaotic motion of the jet and prevented the jet from digressing from the centerline [96].

4 Apparatus and equipments of inkjet printing

With state-of-the-art printing equipments, flexible electronic devices with different scales can be patterned directly. The complexity of inkjet printing techniques stems from several levels of co-optimization of processes and materials. Firstly, the inkjet system has to be integrated including the travel speed of the substrate, the digital data loading and the firing of PZT. In addition, the control system also needs to accommodate corrections for shrinkage and distortions of the flexible substrate [116]. Secondly, the drop size of the ejected ink depends on the viscosity and surface tension of the ink as well as the nozzle dimensions [26,34]. However, since drops need to overlap to form a continuous feature, the rate of firing and the substrate travel speed need to be optimized for high resolution. Finally, the physical and chemical features of the nozzle, ink and substrate have to be optimized to ensure the printabilities of polymer, including the jettable ink, the nozzle without clogging, drops with similar diameter, and the jetted material able to adhere to the substrate [78].

4.1 Conventional inkjet printing systems

Many examples can be found that ordinary desktop color inkjet printers were successfully used for printing polymer solutions. For example, Bhatti et al. [117] fabricated PZT pillars by IBM Colorjet. Gou et al. [118] fabricated PAH/PAA layers by Epson Stylus Color 670 inkjet printer. Kordas et al. [119] fabricated conductive patterns by Cannon BJC 4550. Yoshioka et al. [120] fabricated OLED by Hewlett Packard (HP 5550) thermal desktop inkjet printer. The above equipments are compared in Table 4. Although desktop color inkjet printers are a low cost, available, usage saving apparatus, the average resolution is about 20 μm. In addition, desktop color inkjet printers suffer from several disadvantages when used for printing polymers and nonparticles [37]. Compared conventional pizelectric and thermal bubble method, dispensers have attracted more attention in industry. The dispenser firstly was adopted in aerosol deposition in package. Comparison is given in Table 5, where we just illustrate new development in recent years in dispenser.

The similar microdrop print systems are supplied by many other instrument Incs, such as Litrex, Nano-plotter, GeSim. These apparatuses can combine a camera system to observe the formation of drop by custom option or directly fixing on it. The following is very important for the next generation of inkjet dispenser: (1) Nozzle design: The minimum inner diameter of nozzle should be below 20 μm to create drops with sub-1 pL. Meanwhile, the number of nozzles should be increased in order to enhance yield. (2) *xyz* motion stage design: The position accuracy used in dispenser is about ±5 μm, and the positioning repeatability is about ±1 μm. These stages are based on ball screw and servo control. If the resolution can be enhanced in drop dimension, the stage can adopt linear motor. More information can refer to [121].

4.2 Experiment setups of EHD printing

Presently, EHD print platforms are only in laboratory. Many challenges have to be solved before commercialization. We

Table 4 Instrumentation for conventional inkjet printing

Apparatus	Standard workspace	Print rate	Working temperature	High resolution
Epson Stylus Color 670	A4	5 ppm	Room temperature	720×1440 dpi
Cannon BJC 4550	A4	5 ppm	Room temperature	720×360 dpi
Hewlett packard (HP 5550)	A4	28 ppm	15–27°C	600×600 dpi

Table 5 Instrumentation for polymer inkjet dispensers printing

Apparatus	Workspace (mm×mm)	Accuracy (μm)	Drop volume (pL)	Nozzles	Frequency (kHz)
Microfab Jetlab- II	150×150, 200×200 Option:custom	±15 Option: ±3 with maping	5–500[a)]	4	20
Microfab Jetlab-4	160×120, 210×275 Option:custom	±30, unidirectional	5–500[a)]	4	20
FUJIFILM DMP-3000	300×300	±5	1–10[b)]	128[c)]	10/15[c)]
LP50 inkjet printer	A4	±5	12–25[d)]	128	25
*Microdrop, MD-P-802+AD-K-401	200×200	±5	20–180	1	20

a) Ph-46 drop on demand print head; b) DMP Cartridge-based printheads; c) SX3 head, SE3head; d) print head:PL128-H; *: Autodrop Professional Positioning System MD-P-802 and AD-K-401 combined a system.

will introduce some typical apparatus and critical technologies for bridging the gap between lab-scale and industrial-scale.

(i) Experiment setup of EHD inkjet. Several platform and prototype have been built at the laboratory scale. The main challenge is related with the facts that only at particular flow rates and high-voltage electric field a cone-jet configuration with uniform droplet size can be obtained. Rogers et al. [85] developed a novel high-resolution jet printing system and used this system to study the relationship between the internal diameter of nozzle and the dot diameter and line width. The experimental setup includes a syringe pump (flow rates $\leqslant$ 30 pls^{-1}) or pneumatic pressure controller (applied pressure $\leqslant$ 5 psi), a gold-coated nozzle, a power supply and the substrate/electrode combination mounted on a five-axis (*x*, *y*, *z* axes and two tilting axes in the *x*-*y* plane) stage, shown in Figure 24. These components are connected by pipe and other fixing accessories. They illustrated that high-resolution metal interconnection, electrodes and probing pads for representative circuit patterns and functional transistors with critical dimensions are built as small as 1 μm. Their future wok focused in how to enable this system resolution into nano-scale and enhance the speeds for printing. They illustrated a future EHD inkjet system consisting of *xyz* motion stage and the nozzle fixed in *z* motion stage. The compact multi-nozzle is connected to a syringe pump.

Other groups developed platforms based on the same constitution for different research purpose. Chen et al. [122] described an experimentally validated model for electrically pulsed jets. Lee et al. [112] developed an addressable multi-nozzle to reduce the interference and distortion in the electric field (Figure 25). The multi-nozzle consists of three single nozzles with 360 μm inner diameter and 1100 μm outer diameter, and the distance between adjacent nozzles was 2100 μm. In order to prevent wetting of the silver nanocolloid solution, the telflon was coated in inner surface of nozzle. This new nozzle was proven that interference and distortion did not happen in jet emitting. The cone-jet was so stable even nozzle was revolved. At the same time, all the nozzles can form a symmetric cone-jet mode than pin shaped nozzle. This nozzle can reduce positioning error that's useful to multi-layer deposition.

(ii) Experiment setup of electrospray. This technology is adopted as a nanotechnology only recently. The apparatus is currently at the laboratory scale. Jaworek et al. [123] developed a muti-nozzle electrospray system. Ju et al. [124] fabricated OLED by electrospray deposition (Figure 26). The tip diameter of the glass capillary is 20 μm. The distance between the glass capillary and the glass ITO substrate is 4 cm. There are a maximum 5 kV high-voltage power supply and an acrylic chamber (20 cm × 20 cm × 15 cm). This system can deposit film with 10–200 nm thick-

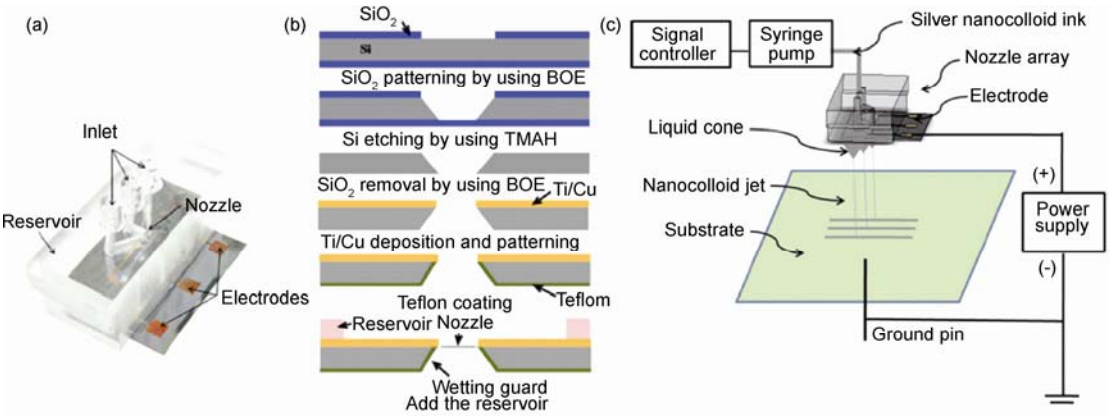

Figure 25 Diagram of structure of multi-nozzle and EHD inkjet system [112]. (a) Fabricated multinozzle and; (b) fabrication flow chart of the multinozzle; (c) schematic of the EHDP system.

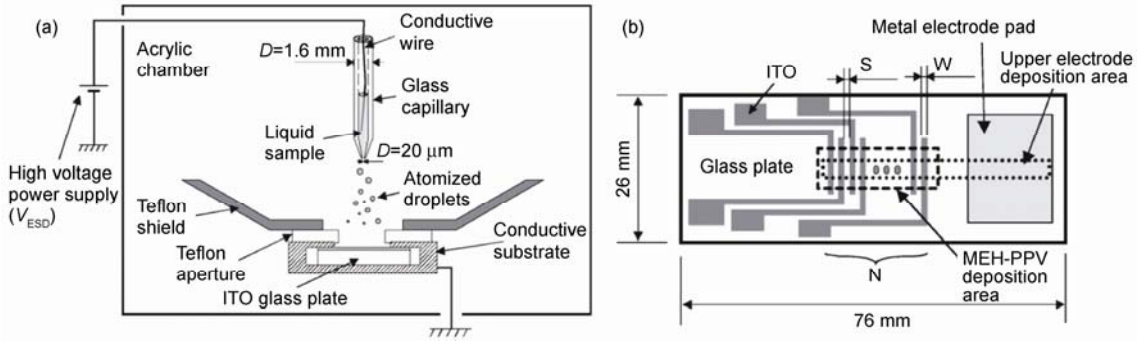

Figure 26 Apparatus and devices used for the fabrication of OLED thin films using electrospray deposition. (a) Apparatus configuration; (b) layout of substrate used for deposition [124].

ness and 100 μm width by spray voltage 2.5–4 kV.

(iii) Experiment setup of electrospinning. An electrospinning system has been developed by IMET Inc and basically consists of a transparent cabin, a high voltage supply and a control module, as shown in Figure 27. The cabin provides a safe and controlled environment for a variety of electrospinning experiments. This apparatus have been applied successfully in various research projects at the Eindhoven University of Technology and the KU leuven. A climate control system has been developed for this apparatus. The current prototype design can control cabin temperature in the range of 15–50°C and humidity in range of 10%–90%. Different techniques are developed for a much higher level of fibre oriented, which depend on producing electrodes and mesh collectors with a predefined 2D or 3D structure.

The industrial nanofiber production equipments are supplied by Elmarco (Nanospider™ technology) with ease of use, scalability, modularity and flexibility in producing the highest quality nanofibers. There are three different types of its production, NS Lab, NS Pilot Line and NS line, shown in Figure 28. The NS Lab 200 and NS Lab 500 are designed with scalability and transition to production (Table 6). The NS Line is a production line can be applied in industrial production. The NS Lab has four interchangeable free spinning electrodes. It has a small volume electrode 'post' (200 mL), ideal for work with novel polymers. NS pilot is ideally suited for new products and low to moderate volume applications. It is a bridge between NS Lab and NS Pilot Line. Their differences are only is voltage and workspace. The serials last product is unwoven fabric, and the fibre is disorder. It can also add some drum collector. Another feature is no spinneret. There are two United State patents [125, 126] similar with Elmarco, providing a high yield nanofibre apparatus with muti-nozzle.

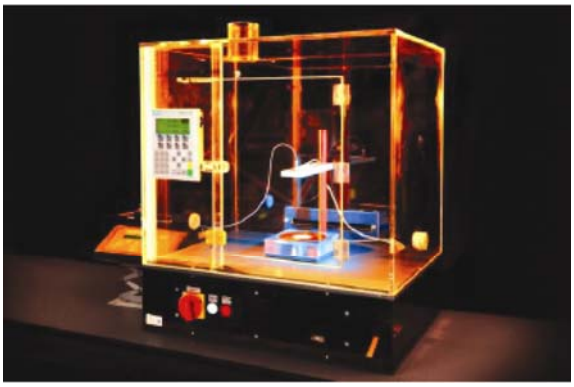

Figure 27 Electrospinning apparatus of IMET (http://www.imetechnologies.nl/).

4.3 R2R web handing for flexible electronics fabrication

The current method of producing electronic devices such as display panels, circuit boards is a batch process using conventional vacuum deposition and lithography pattern technologies on silicon wafers or glass substrates. Flexible electronics, in principle, are amendable to a R2R manufacturing process which represents a dramatic deviation from the current batch process. R2R processing offers a significant advantage compared with the conventional batch process, as it increases throughput by allowing for greater levels of automation and by eliminating the overhead time and human handling involved in loading/unloading panels and processing the substrates [93]. If and when R2R processing technology is adopted in flexible electronics manufacturing, it promises to reduce capital equipment costs, significantly increase throughput. R2R fabrication facility costs scale roughly as the width of the web rather than as the area of the electronics [1]. For large-area devices, this advantage becomes increasingly important.

How to bridge up EHD printing and R2R web system is a big challenge. Figure 29 illustrates a R2R system used in manufacturing a novel electrode of display pixels [127]. In this system, bottom film experiences flexography, drying, vacuum sputter, lift-off, gravure printing and top film ex-

Figure 28 NS Lab and NS Pilot Line system (http://www.elmarco.com/).

Table 6 NS Lab and NS Pilot Line system

Series	Voltage (kV)	Collector height (mm)	Substrate speed (m/min)	Electrode rotation speed (r/min)	Productivity (g/min)	Working environment (°C)	Mininum fibre diameter (nm)
NS Lab	0–80	60–210	0.10–1.56	1–16	1	18–30	80×(1%±30%)
NS Pilot	0–80[a)] 0–60[a)]	100–250	0.20–5	1–16	3	18–40	80×(1%±30%)

a) Spinning heads positive(0–80 kV), Collecting electrode negative(0–60 kV).

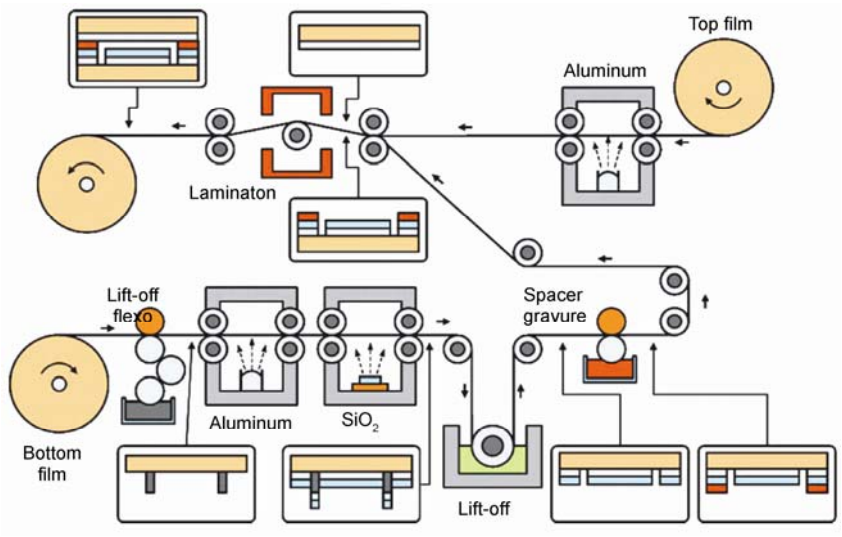

Figure 29 Developing R2R manufacturing system [127].

periences vacuum sputter. Then, the two films were laminated together. In the process, the layer is 1–2 μm by flexography, Al and SiO_2 layers is less than 500 nm. Various layers were printed in different processes and switched for different sequence. Recently, several flexible electronics manufacturing approach has combined with R2R successfully. Hyun et al. [128] exploits the R2R nanoimprint lithography system shown in Figure 30. The system consisted of three units: coating processes, imprinting process and metal deposition process. Polymer patterns are about 70 nm feature size.

Jain et al. [129] developed R2R Lithography systems for flexible displays (Figure 31), a conventional lithography embedded in R2R. These systems meet all of the requirements of patterning on continuous, flexible substrates with high-resolution. The resolution can attain 10 μm. An alignment system ensures a layer-to-layer overlay accuracy of ±2.5 μm. Another system named Anvik HexScanTM 1010 SDE microlithography system, whose resolution is 1 μm and overlay accuracy is ±0.3 μm. Confocal microscopes and a laser interferometer system are integrated into the optical metrology system. In one word, the key manufacturing technologies are high-resolution, R2R, projection lithography and photoablation processing technologies for high-throughput production.

There are some other suitable machine and process for inkjet printing by US Display Consortium project. A good review about R2R manufacturing of flexible displays was also given by Gregg et al. [4]. In these literatures, R2R systems were combined with different patterning technology, including conventional lithograph, flexography, vacuum coating and nanoimprint. When combining these technologies, it must be sure that they are compatible. That means that the resolution and speed of R2R and patterning technology are accordingly suitable. The R2R system must pursue high resolution, high speed and high compatibility. The

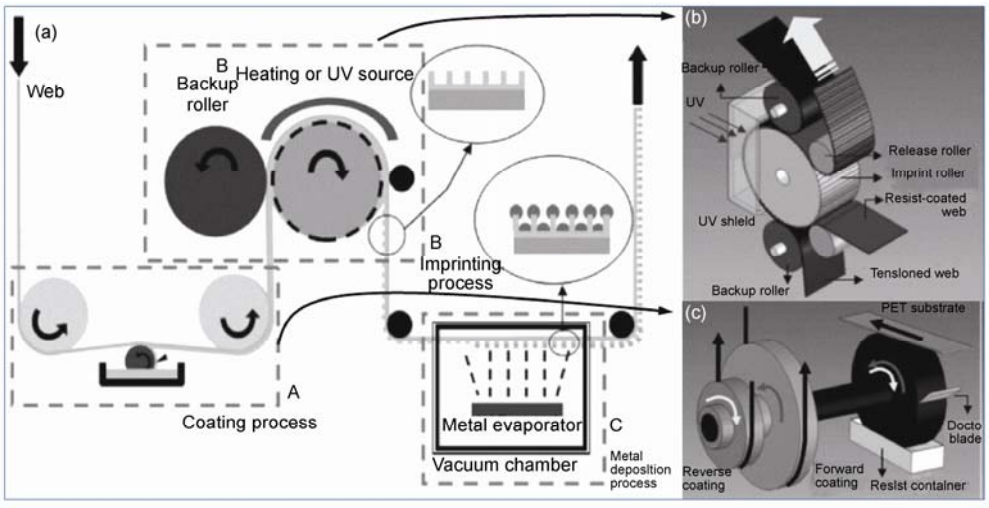

Figure 30 The future and challenge for industry application. (a) Schematic of the R2RNIL; (b) imprint unit; (c) coating unit [128].

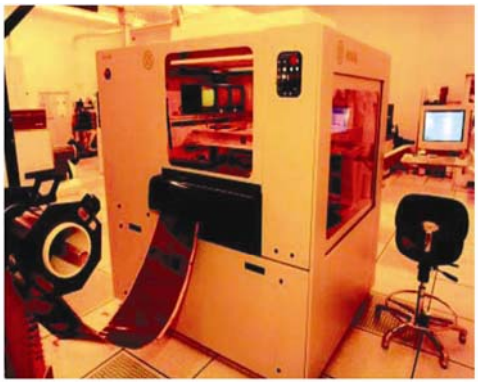

Figure 31 HexScanTM 3100 SRE [129].

critical problem is that the deformation of thin substrates in manufacturing. Another aspect that should be considered is how to eliminate the distortion of web. Several aspects should be considered including tension control, dancer compensation system, layer-to-layer registration, mechanical design. Current research includes: transferring the current processes from glass substrates to R2R processes or developing a new technologies available for R2R processes [93]. EHD printing is a relatively new, powerful and robust processing for direct writing of flexible electronics and nanoelectronics. No matter what types of EHD printing, their efficiency is relative low. Some critical technology to integrate EHD printing with R2R should be improved in industrial application.

5 Challenges and future trends

Flexible electronics are not simply a substitute for existing integrated circuit based electronics products but rather to create new markets [32]. Their functionality and economics are very different from integrated circuits. Inkjet technology has proven to be very effective as a precision manufacturing method. However, the market for printed electronics is in its early stages. Inkjet printing is not a single process but a diverse, versatile and multi-length scale group of process technologies, and a variety of mechanisms and energy modes are used to create material transfer to produce features from nm to mm range [1]. However, there are many challenges in inkjet printing for flexible electronics.

(1) Mechanism of droplet manipulation. Surface/interfacial effects, especially in nanoscale, play important roles in the formation of the cone, deposition of thin film with good morphology, interfacial strength between different layers, even the performance of organic TFTs. It is difficult in understanding how surface/interfacial effects affect the above. Multi-field relates with surface/interfacial effects, which further determine the dynamic behaviors of inkjet printing, such as solidification, deformation, ballistic trajectory, uniformity, then affect the performance of flexible electronics. When particulate or pigmented inks are used, they tend to form non-uniform structures, rather like a coffee stain (Marangoni effect). This makes the understanding of the physics and chemistry involved in the precise manipulation of liquid jets and drops ever more important.

(2) Design of inkjet printer. The structure and the number of nozzle are a bottle neck. In order to gain more yield, the multi-nozzle must be applied. How to form symmetric and stable cone jet is very difficult. In addition, with the inner diameter reducing, the fabrication becomes difficult. The physics and chemistry of the nozzle has to be optimized to ensure the printability of polymer, including the wettability of the inside and outside of the capillary tube, the jettability of ink.

(3) Functional material for inkjetting. Structure at both molecular- and nano-scale impact attributes such as morphology, adhesion, mechanical integrity, solubility, and chemical and environmental stability. These factors, in turn, affect device performance. In addition to mobility, on-off voltage, threshold voltage stability and off current, several other physical and chemical properties play critical roles in inkjet printing, such as viscosity, surface tension, adhesion to a substrate, etc. How to get a material meeting these requirements is a challenge.

(4) Multi-technology integrated by R2R. Many manufacturing methods have been combined, for example, imprint, vacuum deposition, lamination and so on. Generally, different devices require different fabrication process and materials. Firstly, for example, solar cell needs uniform thin film, TFT needs high-resolution line width and uniform structure, sensors and MEMS need more complex patterns. Secondly, many materials are adopted in one component. The designer must be sure that they are compatible and arrange these methods reasonable.

This work was supported by the National Natural Science Foundation of China (50705035 and 50625516) and National Basic Research Program of China (2009CB724204).

1 Wong W S, Salleo A. Flexible Electronics: Materials and Applications. New York: Springer, 2009
2 Reuss R H, Chalamala B R, Moussessian A, et al. Macroelectronics: Perspectives on technology and applications. P IEEE, 2005, 93: 1239–1256
3 Kim D H, Ahn J H, Choi W M, et al. Stretchable and foldable silicon integrated circuits. Science, 2008, 320: 507–511
4 Crawford G P. Flexible Flat Panel Displays. Chichester: John Wiley & Sons, Ltd, 2005
5 Jang J. Displays develop a new flexibility. Mater Today, 2006, 9: 46–52
6 Krebs F C. Fabrication and processing of polymer solar cells: A review of printing and coating techniques. Sol Energy Mater Sol Cells, 2009, 93: 394–412
7 Mayer A C, Scully S R, Hardin B E, et al. Polymer-based solar cells. Mater Today, 2007, 10: 28–33
8 Someya T, Kato Y, Sekitani T, et al. Conformable, flexible, large-area networks of pressure and thermal sensors with organic transistor active matrixes. Proc Natl Acad Sci USA, 2005, 102: 12321–12325

9 Madden P G A. Development and modeling of conducting polymer actuators and the fabrication of a conducting polymer based feedback loop. Cambridge: Massachusetts Institute of Technology, 2003
10 Kim D H, Rogers J A. Stretchable electronics: Materials strategies and devices. Adv Mater, 2008, 20: 4887–4892
11 Park S I, Ahn J H, Feng X, et al. Theoretical and experimental studies of bending of inorganic electronic materials on plastic substrates. Adv Funct Mater, 2008, 18: 2673–2684
12 Khang D Y, Jiang H, Huang Y, et al. A stretchable form of single-crystal silicon for high-performance electronics on rubber substrates. Science, 2006, 311: 208–212
13 Jiang H, Khang D Y, Song J, et al. Finite deformation mechanics in buckled thin films on compliant supports. Prol Natl Acad Sci USA, 2007, 104: 15607–15612
14 Lacour S P, Chan D, Wagner S, et al. Mechanisms of reversible stretchability of thin metal films on elastomeric substrates. Appl Phys Lett, 2006, 88: 204103
15 Sun Y, Choi W M, Jiang H, et al. Controlled buckling of semiconductor nanoribbons for stretchable electronics. Nat Nanotechnology, 2006, 1: 201–206
16 Huang Z Y, Hong W, Suo Z. Nonlinear analyses of wrinkles in a film bonded to a compliant substrate. J Mech Phys Solids, 2005, 53: 2101–2118
17 Jiang H, Sun Y, Rogersc J A, et al. Post-buckling analysis for the precisely controlled buckling of thin film encapsulated by elastomeric substrates. Int J Solids Struct, 2008, 45: 2014–2023
18 Wagner S, Lacour S P, Jones J, et al. Electronic skin: Architecture and components. Physica E, 2004, 25: 326–334
19 Gleskova H, Cheng I C, Wagner S, et al. Mechanics of thin-film transistors and solar cells on flexible substrates. Sol Energy, 2006, 80: 687–693
20 Lacour S P, Wagner S, Huang Z, et al. Stretchable gold conductors on elastomeric substrates. Appl Phys Lett, 2003, 82: 2404–2406
21 Xu W, Lu T. Flexible electronics system and their mechanical properties (in Chinese). Adv Mech, 2008, 48: 137–150
22 Huang Y, Yin Z, Xiong Y. Thermomechanical analysis of film-on-substrate system with temperature-dependent properties. J Appl Mech-T ASME, 2010, 77: 1–9
23 Huang Y, Yin Z, Xiong Y. Thermomechanical analysis of thin films on temperature-dependent elastomeric substrates in flexible heterogeneous electronics. Thin Solid Films, 2010, 518: 1698–1702
24 Logothetidis S. Flexible organic electronic devices: Materials, process and applications. Mater Sci Eng B, 2008, 152: 96–104
25 de Gans B J, Duineveld P C, Schubert U S. Inkjet printing of polymers: State of the art and future developments. Adv Mater, 2004, 16: 203–213
26 Menard E, Meitl M A, Sun Y G, et al. Micro- and nanopatterning techniques for organic electronic and optoelectronic systems. Chem Rev, 2007, 107: 1117–1160
27 Calvert P. Inkjet printing for materials and devices. Chem Mater, 2001, 13: 3299–3305
28 Lan H, Ding Y, Liu H, et al. Review of template fabrication for nanoimprint lithography (in Chinese). J Mech Eng, 2009, 45: 1–13
29 Sirringhaus H, Kawase T, Friend R H, et al. High-resolution inkjet printing of all-polymer transistor circuits. Science, 2000, 290: 2123–2126
30 Wang Y, Bokor J, Lee A. Maskless lithography using drop-on-demand inkjet printing method. P Soc Photo-Opt Ins, 2004, 5374: 628–636, 1110
31 Singh T B, Sariciftci N S. Progress in plastic electronics devices. Annu Rev Mater Res, 2006, 36: 199–230
32 Kelley T W, Baude P F, Gerlach C, et al. Recent progress in organic electronics: Materials, devices, and processes. Chem Mater, 2004, 16: 4413–4422
33 Reichmanis E, Katz H, Kloc C, et al. Plastic electronic devices: From materials design to device applications. Bell Labs Tech J, 2005, 10: 87–105
34 Jang D, Kim D, Moon J. Influence of fluid physical properties on ink-jet printability. Langmuir, 2009, 25: 2629–2635
35 Bergeron V, Bonn D, Martin J Y, et al. Controlling droplet deposition with polymer additives. Nature, 2000, 405: 772–775
36 Martin G D, Hoath S D, Hutchings I M. Inkjet printing-the physics of manipulating liquid jets and drops. J Phys: Conf Ser, 2008, 105: 012001–012014
37 de Gans B J, Schubert U S. Inkjet printing of polymer micro-arrays and libraries: Instrumentation, requirements, and perspectives. Macromol Rapid Comm, 2003, 24: 659–666
38 Mabrook M F, Pearson C, Jombert A S, et al. The morphology, electrical conductivity and vapour sensing ability of inkjet-printed thin films of single-wall carbon nanotubes. Carbon, 2009, 47: 752–757
39 Fan Z J, Wei T, Luo G H, et al. Fabrication and characterization of multi-walled carbon nanotubes-based ink. J Mater Sci, 2005, 40: 5075–5077
40 Wei T, Ruan J, Fan Z J, et al. Preparation of a carbon nanotube film by ink-jet printing. Carbon, 2007, 45: 2712–2716
41 Song J W, Kim Y S, Yoon Y H, et al. The production of transparent carbon nanotube field emitters using inkjet printing. Physica E, 2009, 41: 1513–1516
42 Dror Y, Salalha W, Khalfin R L, et al. Carbon nanotubes embedded in oriented polymer nanofibers by electrospinning. Langmuir, 2003, 19: 7012–7020
43 Zhang Q H, Chang Z J, Zhu M F, et al. Electrospun carbon nanotube composite nanofibres with uniaxially aligned arrays. Nanotechnology, 2007, 18: 115611–115616
44 Magdassi S, Bassa A, Vinetsky Y, et al. Silver nanoparticles as pigments for water-based ink-jet inks. Chem Mater, 2003, 15: 2208–2217
45 Lee H H, Chou K S, Huang K C. Inkjet printing of nanosized silver colloids. Nanotechnology, 2005, 16: 2436–2441
46 Perelaer J, de Gans B J, Schubert U S. Ink-jet printing and microwave sintering of conductive silver tracks. Adv Mater, 2006, 18: 2101–2104
47 Dearden A L, Smith P J, Shin D Y, et al. A low curing temperature silver ink for use in ink-jet printing and subsequent production of conductive tracks. Macromol Rapid Comm, 2005, 26: 315–318
48 Liu Z, Wen F S, Li W L. Synthesis and electroluminescence properties of europium(III) complexes with new second ligands. Thin Solid Films, 2005, 478: 265–270
49 Park B K, Kim D, Jeong S, et al. Direct writing of copper conductive patterns by ink-jet printing. Thin Solid Films, 2007, 515: 7706–7711
50 Woo K, Kim D, Kim J S, et al. Ink-jet printing of Cu-Ag-based highly conductive tracks on a transparent substrate. Langmuir, 2009, 25: 429–433
51 Kamyshny A, Ben-Moshe M, Aviezer S, et al. Ink-jet printing of metallic nanoparticles and microemulsions. Macromol Rapid Comm, 2005, 26: 281–288
52 Kim D, Moon J. Highly conductive ink jet printed films of nanosilver particles for printable electronics. Electrochem Solid ST, 2005, 8: J30–J33
53 Hsu S L C, Wu R T. Synthesis of contamination-free silver nanoparticle suspensions for micro-interconnects. Mater Lett, 2007, 61: 3719–3722
54 Wu R T, Hsu S L C. Preparation of highly concentrated and stable suspensions of silver nanoparticles by an organic base catalyzed reduction reaction. Mater Res Bull, 2008, 43: 1276–1281
55 Wu J T, Hsu S L C, Tsai M H, et al. Conductive silver patterns via ethylene glycol vapor reduction of ink-jet printed silver nitrate tracks on a polyimide substrate. Thin Solid Films, 2009, 517: 5913–5917
56 Lee D Y, Shin Y S, Park S E, et al. Electrohydrodynamic printing of silver nanoparticles by using a focused nanocolloid jet. Appl Phys Lett, 2007, 90: 0819051–0819053
57 Lee D Y, Lee J C, Shin Y S, et al. Structuring of conductive silver line by electrohydrodynamic jet printing and its electrical characterization. J Phys: Conf Ser, 2007, 142: 012039

58 Chronakis I S, Grapenson S, Jakob A. Conductive polypyrrole nanofibers via electrospinning: Electrical and morphological properties. Polymer, 2006, 47: 1597–1603
59 Shen W F, Zhao Y, Zhang C B. The preparation of ZnO based gas-sensing thin films by ink-jet printing method. Thin Solid Films, 2005, 483: 382–387
60 Choi J H, Khang D Y, Myoung J M. Fabrication and characterization of ZnO nanowire transistors with organic polymer as a dielectric layer. Solid State Commun, 2008, 148: 126–130
61 Yang Y J, Jiang Y D, Xu J H, et al. Conducting PEDOT-PSS composite films assembled by LB technique. Colloid Surface A, 2007, 302: 157–161
62 Jang J, Chang M, Yoon H. Chemical sensors based on highly conductive poly(3,4-ethylenedioxythiophene) nanorods. Adv Mater, 2005, 17: 1616–1620
63 Ballarin B, Fraleoni-Morgera A, Frascaro D, et al. Thermal inkjet microdeposition of PEDOT: PSS on ITO-coated glass and characterization of the obtained film. Synthetic Met, 2004, 146: 201–205
64 Eom S H, Senthilarasu S, Uthirakumar P, et al. Polymer solar cells based on inkjet-printed PEDOT:PSS layer. Org Electron, 2009, 10: 536–542
65 Hohnholz D, Okuzaki H, MacDiarmid A G. Plastic electronic devices through line patterning of conducting polymers. Adv Funct Mater, 2005, 15: 51–56
66 Kwon I W, Son H J, Kim W Y, et al. Thermistor behavior of PEDOT: PSS thin film. Synthetic Met, 2009, 159: 1174–1177
67 Jeong S, Kim D, Moon J. Ink-jet-printed organic-inorganic hybrid dielectrics for organic thin-film transistors. J Phys Chem C, 2008, 112: 5245–5249
68 Xie X L, Mai Y W, Zhou X P. Dispersion and alignment of carbon nanotubes in polymer matrix: A review. Mat Sci Eng R, 2005, 49: 89–112
69 Lin H W, Hwu W H, Ger M D. The dispersion of silver nanoparticles with physical dispersal procedures. J Mater Process Tech, 2008, 206: 56–61
70 Hon K K B, Li L, Hutchings I M. Direct writing technology- Advances and developments. Cirp Ann-Manuf Techn, 2008, 57: 601–620
71 Le H P. Progress and trends in ink-jet printing technology. J Imaging Sci Techn, 1998, 42: 49–62
72 Paul K E, Wong W S, Ready S E, et al. Additive jet printing of polymer thin-film transistors. Appl Phys Lett, 2003, 83: 2070–2072
73 Wang Y, Bokor J. Ultra-high-resolution monolithic thermal bubble inkjet print head. J Micro-Nanolith Mem, 2007, 6: 043009
74 Dong H M, Carr W W, Morris J F. An experimental study of drop-on-demand drop formation. Phys Fluids, 2006, 18: 0721021–0721016
75 Noguchi Y, Sekitani T, Yokota T, et al. Direct inkjet printing of silver electrodes on organic semiconductors for thin-film transistors with top contact geometry. Appl Phys Lett, 2008, 93: 0433031–0433033
76 Duineveld P C. The stability of ink-jet printed lines of liquid with zero receding contact angle on a homogeneous substrate. J Fluid Mech , 2003, 477: 175–200
77 Lim J A, Lee H S, Lee W H, et al. Control of the morphology and structural development of solution-processed functionalized acenes for high-performance organic transistors. Adv Funct Mater, 2009, 19: 1515–1525
78 Roy S. Fabrication of micro- and nano-structured materials using mask-less processes. J Phys D Appl Phys, 2007, 40: R413–R426
79 Sirringhaus H, Kawase T, Friend R H. High-resolution ink-jet printing of all-polymer transistor circuits. MRS Bull, 2001, 26: 539 –543
80 Li S P, Newsome C J, Kugler T, et al. Polymer thin film transistors with self-aligned gates fabricated using ink-jet printing. Appl Phys Lett, 2007, 90: 1721031–1721033
81 Noh Y Y, Zhao N, Caironi M, et al. Downscaling of self-aligned, all-printed polymer thin-film transistors. Nat Nanotechnol, 2007, 2: 784–789
82 Bao Z N. Fine printing. Nat Mater, 2004, 3: 137–138
83 Sele C W, von Werne T, Friend R H, et al. Lithography-free, self-aligned inkjet printing with sub-hundred-nanometer resolution. Adv Mater, 2005, 17: 997–1001
84 Ko S H, Pan H, Grigoropoulos C P, et al. All-inkjet-printed flexible electronics fabrication on a polymer substrate by low-temperature high-resolution selective laser sintering of metal nanoparticles. Nanotechnology, 2007, 18: 3452021–3452028
85 Park J U, Hardy M, Kang S J, et al. High-resolution electrohydrodynamic jet printing. Nat Mater, 2007, 6: 782–789
86 Jaworek A, Sobczyk A T. Electrospraying route to nanotechnology: An overview. J Electrostat, 2008, 66: 197–219
87 Kim J, Oh H, Kim S S. Electrohydrodynamic drop-on-demand patterning in pulsed cone-jet mode at various frequencies. J Aerosol Sci, 2008, 39: 819–825
88 Basaran O A. Small-scale free surface flows with breakup: Drop formation and emerging applications. Aiche J, 2002, 48: 1842-1848
89 Jaworek A, Krupa A. Classification of the modes of EHD spraying. J Aerosol Sci, 1999, 30: 873–893
90 Paine M D, Alexander M S, Smith K L, et al. Controlled electrospray pulsation for deposition of femtoliter fluid droplets onto surfaces. J Aerosol Sci, 2007, 38: 315–324
91 Li J L. On the meniscus deformation when the pulsed voltage is applied. J Electrostat, 2006, 64: 44–52
92 Teo W E, Ramakrishna S. A review on electrospinning design and nanofibre assemblies. Nanotechnology, 2006, 17: R89–R106
93 Choi J, Kim Y J, Lee S, et al. Drop-on-demand printing of conductive ink by electrostatic field induced inkjet head. Appl Phys Lett, 2008, 93: 1935081–1935083
94 Reneker D H, Yarin A L. Electrospinning jets and polymer nanofibers. Polymer, 2008, 49: 2387–2425
95 Jayasinghe S N, Dorey R A, Edirisinghe M J, et al. Preparation of lead zirconate titanate nano-powder by electrohydrodynamic atomization. Appl Phys A Mater, 2005, 80: 723–725
96 Jaworek A. Electrospray droplet sources for thin film deposition. J Mater Sci, 2007, 42: 266–297
97 Saf R, Goriup M, Steindl T, et al. Thin organic films by atmospheric-pressure ion deposition. Nat Mater, 2004, 3: 323–329
98 Salata O V. Tools of nanotechnology: Electrospray. Curr Nanosci, 2005, 1: 25–33
99 Yu F X, Cui J Z, Ranganathan S, et al. Fundamental differences between spray forming and other semisolid processes. Mat Sci Eng A-Struct, 2001, 304: 621–626
100 Chen X, Cheng J, Yin X. Advances and applications of electrohydrodynamics. Chinese Sci Bull, 2003, 48: 1055-1063
101 Fujihara K, Kumar A, Jose R, et al. Spray deposition of electrospun TiO_2 nanorods for dye-sensitized solar cell. Nanotechnology, 2007, 18: 3657091–3657095
102 Cich M, Kim K, Choi H, et al. Deposition of $(Zn,Mn)(2)SiO_4$ for plasma display panels using charged liquid cluster beam. Appl Phys Lett, 1998, 73: 2116–2118
103 Huang Z M, Zhang Y Z, Kotaki M, et al. A review on polymer nanofibers by electrospinning and their applications in nanocomposites. Compos Sci Technol, 2003, 63: 2223–2253
104 MacDiarmid A G. "Synthetic metals": A novel role for organic polymers (Nobel lecture). Angew Chem Int Edit, 2001, 40: 2581 –2590
105 Sun D, Chang C, Li S, et al. Near-field electrospinning. Nano Lett, 2006, 6: 839–842
106 Yarin A L, Zussman E. Upward needleless electrospinning of multiple nanofibers. Polymer, 2004, 45: 2977–2980
107 Hellmann C, Belardi J, Dersch R, et al. High precision deposition electrospinning of nanofibers and nanofiber nonwovens. Polymer, 2009, 50: 1197–1205
108 Fang J, Niu H, Lin T, et al. Applications of electrospun nanofibers. Chinese Sci Bull, 2008, 53: 2265–2286
109 Jeong J S, Jeon S Y, Lee T Y, et al. Fabrication of MWNTs/nylon conductive composite nanofibers by electrospinning. Diam Relat Mater, 2006, 15: 1839–1843

110 Sekitani T, Noguchi Y, Zschieschang U, et al. Organic transistors manufactured using inkjet technology with subfemtoliter accuracy. Prol Natl Acad Sci USA, 2008, 105: 4976–4980

111 Choi H K, Park J U, Park O O, et al. Scaling laws for jet pulsations associated with high-resolution electrohydrodynamic printing. Appl Phys Lett, 2008, 92: 1231091–1231093

112 Lee J S, Kim S Y, Kim Y J, et al. Design and evaluation of a silicon based multi-nozzle for addressable jetting using a controlled flow rate in electrohydrodynamic jet printing. Appl Phys Lett, 2008, 93: 2431141–2431143

113 Yang D, Wang Y, Zhang D. et al. Control of the morphology of micro/nano-structures of polycarbonate via electrospinning. Chinese Sci Bull, 2009, 54: 2911–2917

114 Kim S G, Choi K H, Eun J H, et al. Effects of additives on properties of MgO thin films by electrostatic spray deposition. Thin Solid Films, 2000, 377: 694–698

115 Sorensen G. Ion bombardment of electrosprayed coatings: An alternative to reactive sputtering. Surf Coat Tech, 1999, 112: 221–225

116 Dong H M, Carr W W, Morris J F. Visualization of drop-on-demand inkjet: Drop formation and deposition. Revi Sci Instrum, 2006, 77: 0851011–0851018

117 Bhatti A R, Mott M, Evans J R G, et al. PZT pillars for 1–3 composites prepared by ink-jet printing. J Mater Sci Lett, 2001, 20: 1245–1248

118 Guo T F, Chang S C, Pyo S, et al. Vertically integrated electronic circuits via a combination of self-assembled polyelectrolytes, ink-jet printing, and electroless metal plating processes. Langmuir, 2002, 18: 8142–8147

119 Kordas K, Mustonen T, Toth G, et al. Inkjet printing of electrically conductive patterns of carbon nanotubes. Small, 2006, 2: 1021–1025

120 Yoshioka Y, Jabbour G E. Desktop inkjet printer as a tool to print conducting polymers. Synthetic Met, 2006, 156: 779–783

121 Ding H, Xiong Z. Motion stages for electronic packaging design and control. IEEE Robot Autom Mag, 2006, 13: 51–61

122 Chen C H, Saville D A, Aksay I A. Scaling laws for pulsed electrohydrodynamic drop formation. Appl Phys Lett, 2006, 89: 1241031–1241033

123 Jaworek A, Balachandran W, Lackowski M, et al. Multi-nozzle electrospray system for gas cleaning processes. J Electrostat, 2006, 64: 194–202

124 Ju J, Yamagata Y, Higuchi T. Thin-film fabrication method for organic light-emitting diodes using electrospray deposition. Adv Mater, 2009, 21: 1–5

125 Darty M A. Methods and apparatus for electrohydrodynamic ejection. United States Patent, 2001

126 Lee W S, Jo S M, Go S G, et al. Apparatus of polymer web by electrospinning process. United States Patent, 2003

127 Lo C Y, Hiitola-Keinanen J, Huttunen O H, et al. Novel roll-to-roll lift-off patterned active-matrix display on flexible polymer substrate. Microelectron Eng, 2009, 86: 979–983

128 Ahn S H, Guo L J. High-speed roll-to-roll nanoimprint lithography on flexible plastic substrates. Adv Mater, 2008, 20: 2044–2049

129 Jain K, Klosner M, Zemel M, et al. Flexible electronics and displays: High-resolution, roll-to-roll, projection lithography and photoablation processing technologies for high-throughput production. P IEEE, 2005, 93: 1500–1510